Nanoscale Horizons

ROYAL SOCIETY OF CHEMISTRY

REVIEW

View Article Online
View Journal

Check for updates

Cite this: DOI: 10.1039/d5nh00612k

Covalent organic frameworks as precision nanocarriers for targeted drug delivery: developments, hurdles, and horizons

Tsukasa Irie, Saikat Das * and Yuichi Negishi *

Received 1st September 2025,
Accepted 6th January 2026

DOI: 10.1039/d5nh00612k

rsc.li/nanoscale-horizons

Covalent organic frameworks (COFs) have emerged as a versatile class of crystalline reticular materials distinguished by their high surface area, permanent porosity, and atomically precise structural tunability. Their modular synthesis enables precise control over pore size, geometry, and surface functionality, while offering excellent chemical stability and intrinsic biocompatibility. These attributes make COFs uniquely suited for applications as precision nanocarriers in targeted drug delivery. Recent advances demonstrate that COFs can encapsulate therapeutic agents with high loading efficiency and facilitate controlled, stimuli-responsive release profiles. Furthermore, the incorporation of targeting moieties through linker design or post-synthetic modification enables site-specific delivery, minimizing off-target cytotoxicity and enhancing therapeutic efficacy—particularly in oncological contexts. This review critically evaluates the current landscape of COF-based drug delivery systems, detailing structural design strategies, loading and release mechanisms, and functionalization approaches for precision targeting. We also highlight key challenges—such as scalable synthesis, pharmacokinetics, and *in vivo* stability—and outline promising research directions toward the clinical translation of COF nanocarriers for personalized medicine.

1. Introduction

The efficient delivery of therapeutics remains a central challenge in modern medicine. Despite the discovery of numerous bioactive molecules and small-molecule drugs over the past century, achieving precise spatiotemporal control over drug distribution, bioavailability, and release remains a formidable obstacle. Conventional administration methods often suffer from systemic toxicity, poor pharmacokinetics (PK), off-target effects, and rapid clearance, which limit therapeutic efficacy and necessitate high or frequent dosing. These limitations have driven the emergence of advanced drug delivery systems designed to navigate complex biological barriers, maintain drug stability, and provide controlled and targeted release profiles.[1–10] Controlled drug delivery, a concept formalized in the mid-20th century, initially focused on oral and transdermal systems, employing mechanisms such as diffusion, dissolution, osmosis, and ion exchange to regulate the release of therapeutic agents.[11] Subsequent decades saw the exploration of self-regulating and stimuli-responsive systems capable of dynamically modulating release in response to physiological cues, though technological limitations initially constrained their clinical translation. The 21st century has witnessed a revolution in nanoscale drug carriers, including nanoparticles, liposomes, polymeric micelles, carbon-based nanomaterials, quantum dots, mesoporous silica, and more recently, two-dimensional materials such as MXenes.[12–16] These platforms offer enhanced loading capacities, improved solubility of hydrophobic drugs, and the potential for tumor-targeted delivery *via* the enhanced permeability and retention (EPR) effect, thereby increasing therapeutic efficacy while reducing systemic toxicity.[17] Despite these advancements, each class of drug carrier presents inherent limitations. Inorganic nanocarriers, such as mesoporous silica nanoparticles (MSNs) or quantum dots, can leach residual metal ions, inducing cytotoxicity, oxidative stress, or unintended immune responses.[18,19] Coordination polymers have also gained attention for drug delivery; however, their metal-containing backbones may similarly raise concerns regarding ion release, stability, and long-term biocompatibility.[20] Carbon-based carriers and polymeric nanoparticles often require complex, multi-step syntheses under stringent conditions, elevating costs and limiting scalability.[21] Liposomes and polymeric carriers may suffer from chemical instability in physiological environments, leading to premature drug release and reduced efficacy.[22] Functionalization strategies to impart targeting capabilities often add

Institute of Multidisciplinary Research for Advanced Materials, Tohoku University, 2-1-1 Katahira, Aoba-ku, Sendai 980-8577, Japan.
E-mail: das.saikat.c4@tohoku.ac.jp, yuichi.negishi.a8@tohoku.ac.jp

synthetic complexity and variability. Furthermore, achieving precisely controlled, sustained, or stimuli-responsive drug release remains a persistent challenge across most nanocarrier platforms.[23,24]

These challenges have prompted a search for next-generation materials with exceptional structural tunability, high surface areas, biocompatibility, and controllable porosity. Covalent organic frameworks (COFs), an emerging class of crystalline, extended-structure materials, have attracted significant attention in this context.[25–37] Since their first report in 2005 by Yaghi and co-workers,[38] COFs have been recognized for their modularity, chemical stability, and highly designable architectures. Two-dimensional (2D)[39] and three-dimensional (3D)[40] COFs can be synthesized from a variety of organic building blocks and covalent linkages—including imine, hydrazone, β-ketoenamine, imidazole, amide, phenazine, boronate ester, boroxine, urea, vinylene, among others—allowing precise tuning of pore size, surface chemistry, and functional group density.[41] Several features make COFs particularly well-suited for drug delivery. Their porous frameworks facilitate high drug loading and efficient encapsulation, while the abundance of functional groups enables specific targeting and interaction with biological molecules. The absence of heavy metals reduces toxicity relative to many inorganic carriers, and the structural rigidity and π–π, CH–π, hydrogen bonding, and van der Waals interactions provide stability for drug–COF complexes. Moreover, COFs allow controlled, sustained, and programmable drug release, minimizing premature leakage and enhancing therapeutic efficacy. The versatility of COFs also permits integration with stimuli-responsive components or other nanomaterials to further tailor PK and biodistribution. Collectively, these attributes position COFs as a transformative platform for next-generation drug delivery, bridging the gap between materials chemistry and precision therapeutics (Fig. 1).

This Review provides a comprehensive overview of COFs as nanocarriers, emphasizing how their structure–property relationships influence drug loading, release kinetics, and targeted delivery. It also critically examines the advantages and limitations of existing drug delivery systems and highlights the potential of COFs to overcome current challenges, offering a forward-looking perspective on their role in advancing nanomedicine. In Section 2, we focus on precision therapeutic drug delivery, discussing strategies for targeted and stimulus-responsive release to maximize efficacy while minimizing off-target effects. Section 3 delves into the fundamentals of COFs, detailing different covalent linkages and synthetic methodologies for constructing 2D and 3D frameworks with tunable porosity and functionality. Section 4 reviews recent developments in COFs as competent drug delivery vehicles—highlighting exemplary systems that demonstrate enhanced drug loading, controlled release profiles, biocompatibility, and tumor targeting. Section 5 offers a forward-looking perspective on future challenges and opportunities, including biodegradability, large-scale synthesis, multifunctionality integration, and translation toward clinical applications. Despite the availability of several reviews on COFs for drug delivery,[42–46] our contribution is distinguished by its unique focus and depth. Specifically, our review: (1) systematically compiles and

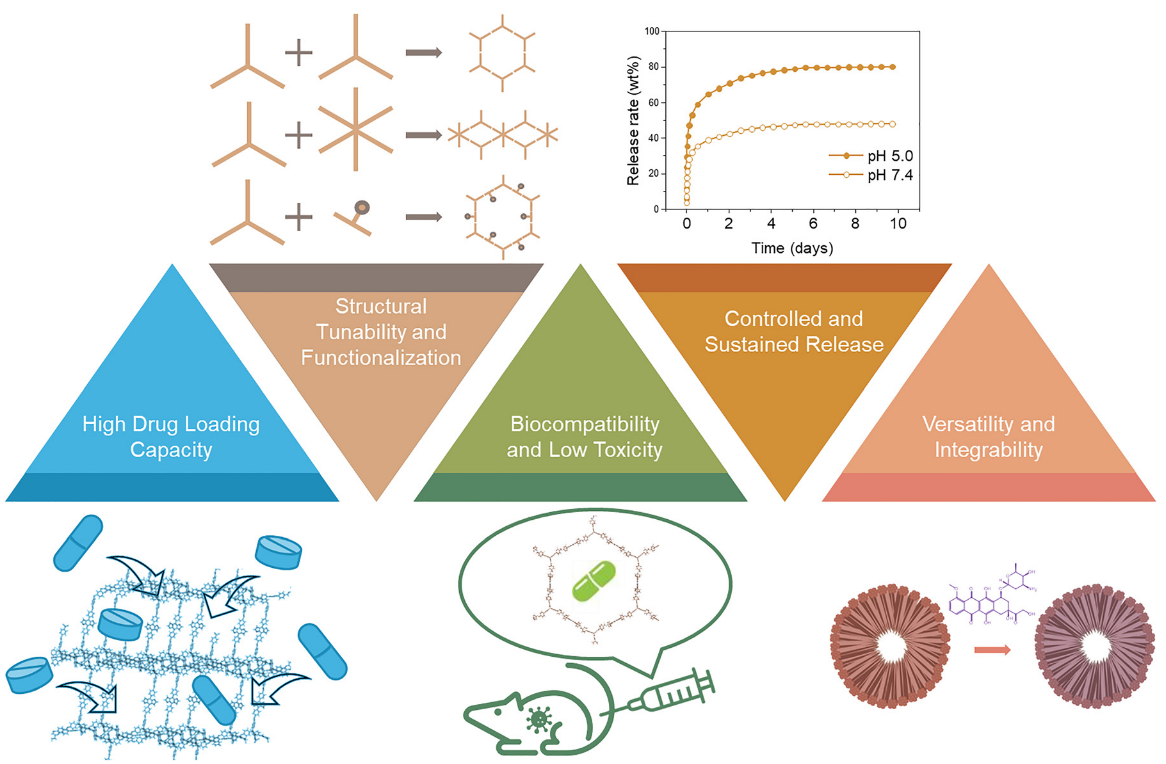

Fig. 1 Key structural and functional attributes of COFs that underpin their utility as drug delivery platforms.

organizes organizes up-to-date reports on drug loading capacities, release behaviors, and biocompatibility of COFs, highlighting general trends while noting the limited structure–performance correlations in the current literature; (2) integrates advances in stimuli-responsive and targeted COF-based systems, extending the discussion to *in vivo* performance and translational relevance; (3) exclusively concentrates on drug delivery, offering detailed treatment of drug encapsulation efficiency, PK, and biocompatibility rather than broader biomedical applications; (4) outlines actionable design principles and future roadmaps for multifunctional COF-based nanocarriers, including prospects for co-delivery and synergistic therapy.

2. Precision therapeutic drug delivery

COFs offer a uniquely powerful platform for precision therapeutic drug delivery through the intersection of tunable porosity, chemical stability, and facile functionalization. Below, we elaborate on key strategies—targeting, stimuli-responsiveness, and controlled loading/release—underpinned by recent advances in COF-enabled delivery systems.

2.1 Engineered targeting through surface and pore environment functionalization

A critical requirement in precision drug delivery is the selective accumulation of therapeutic agents at pathological sites, thereby maximizing efficacy while minimizing systemic toxicity. COFs enable this through the deliberate functionalization of their surfaces or pore interfaces. By integrating targeting ligands—such as antibodies, aptamers, peptides, or small molecules—onto the COF backbone, nanocarriers can exploit receptor–ligand interactions to recognize overexpressed biomarkers on diseased cells, triggering receptor-mediated endocytosis and enhancing the therapeutic index. The modular nature of reticular chemistry allows precise installation of functional handles during the synthesis or *via* post-synthetic modification, ensuring high ligand density and orientation control. Representative strategies include the incorporation of folic acid as a tumor-targeting motif, which exploits folate receptor overexpression on cancer cells,[47] and RGD peptides, which bind integrins with high affinity to direct nanosystems toward integrin-overexpressing cancer cells.[48] Such strategies underscore the ability of COFs to integrate molecular recognition elements within ordered porous architectures, advancing the design of precision nanocarriers for targeted therapy.

2.2 Stimuli-responsive release: controlled and on-demand delivery

Precision delivery not only requires selective targeting but also controlled drug release in response to specific stimuli. COFs stand out in this regard, as they can be rationally engineered to incorporate stimuli-sensitive motifs that ensure spatially and temporally regulated drug release. These triggers can be endogenous—such as the acidic pH of tumor tissues, elevated glutathione (GSH) concentrations in the cytosol, or hypoxic gradients—or exogenous, including light, magnetic fields, temperature, or ultrasound. By embedding labile linkers—such as hydrazone (acid-labile) and disulfide (redox-cleavable) bonds—COFs remain structurally robust under physiological conditions yet undergo rapid disassembly once exposed to tumor-specific environments. This dual stability–responsiveness balance ensures negligible premature leakage during circulation while achieving maximal on-site drug dosing. For instance, PEGylated (PEG = polyethylene glycol) COFs incorporating both hydrazone and disulfide functionalities demonstrated exceptionally high doxorubicin (DOX) loading capacity, negligible drug leakage under physiological conditions, and efficient release under acidic, GSH-rich tumor microenvironments.[49] Such smart release systems exemplify the spatiotemporal precision that COFs can offer, ultimately reducing systemic toxicity and enhancing therapeutic efficacy.

2.3 Mechanisms of drug loading and protection

COFs, with their highly ordered porous architectures, tunable pore sizes, and extensive surface areas, offer versatile platforms for drug encapsulation and stabilization. The mechanisms governing drug loading extend beyond simple physical entrapment to include a spectrum of noncovalent and covalent interactions. π–π interactions between the conjugated COF backbones and aromatic moieties of chemotherapeutic agents *e.g.* 5-fluorouracil and tuberculosis medication *e.g.* isoniazid significantly enhances loading efficiency while mitigating undesired burst release.[50] This principle—leveraging π–π stacking for robust drug loading—has been broadly applied across nanocarrier systems, including carbon-based[51] and porous materials,[52] to achieve high loading capacities and controlled release behavior. Hydrogen bonding, van der Waals forces, and electrostatic interactions between framework linkages and drug functional groups can further contribute to stabilization within the pores.[53] Size- and shape-selective confinement additionally restricts drug mobility, providing another layer of controlled retention. Atomically precise pore architecture in COFs enables tailored confinement to suit specific drug geometries, guiding retention and release kinetics. Beyond loading, COFs can function as protective reservoirs for active pharmaceutical ingredients (APIs), safeguarding them from hydrolytic, enzymatic, or oxidative degradation during systemic circulation. The crystalline rigidity of COFs can hinder drug diffusion until specific biological or external stimuli trigger release, thereby extending circulation half-life and improving PK profiles. Similar protective advantages have been observed in other nanomaterials used for API delivery, emphasizing the broader relevance of this mechanism.[54] Furthermore, COFs' tunable chemical environments—hydrophobic or hydrophilic domains, charged pore interiors, or stimuli-responsive functional groups—allow tailored host–guest interactions for different classes of therapeutics. This structural versatility supports the selective encapsulation and controlled delivery of APIs with varied properties. Collectively, these multifaceted mechanisms not only enhance drug payload and stability but also maximize bioavailability and therapeutic efficacy while minimizing off-target effects.

2.4 Tunable porosity and morphology for optimized loading, release, and cellular performance

Control over pore size, geometry, and topology enables bespoke matching of a COF's architecture to its intended cargo. Fine-tuning these structural parameters allows systematic optimization of loading capacity and release kinetics, striking a crucial balance between surface area and pore accessibility. Thoughtful design of pore dimensions ensures effective encapsulation—too small, and the therapeutic agent may be excluded; too large, and framework stability or controlled release may be compromised. Rational pore engineering thus serves as a versatile strategy to adapt COF platforms for a broad range of pharmaceutical agents.

Beyond internal porosity, the external morphology of COF nanoparticles—including forms such as nanospheres, nanosheets, nanorods, and hollow capsules—profoundly affects their biological performance. These shape variations modulate: (a) cellular uptake pathways and kinetics: for example, in non-COF systems, simulations have demonstrated that spherical nanoparticles are internalized more rapidly than rod- or disk-shaped analogues, largely due to lower membrane-bending energy requirements during endocytosis.[55] (b) Biodistribution and organ targeting: studies with non-spherical nanoparticles indicate that discoidal particles preferentially accumulate in lungs and spleens, while cylindrical shapes tend to localize more in the liver.[56] Although analogous detailed studies are still evolving within the COF domain, emerging research illustrates the promise of morphology-controlled COF designs. A particularly illustrative example is the development of hollow nanosphere COFs (HCOFs) using silica core–shell templates.[57] These 2D hollow structures, with high surface areas (2087 m^2 g^{-1}), achieve exceptional drug loading (99.6%) and display superior tumor accumulation—likely due to their well-defined morphology and shell architecture. These findings underscore that the design of COFs requires careful consideration of tunable porosity for optimal drug compatibility alongside morphological control to enhance cellular internalization and biodistribution. Integrating these design levers can significantly improve COF-based nanocarriers' therapeutic efficacy and precision.

2.5 Multi-modal theranostics: converging therapy and imaging

COFs accommodate multifunctional payloads—including therapeutics, imaging dyes, and photothermal agents—within a single, cohesive platform, thereby enabling true theranostic applications. By embedding fluorophores or contrast agents, COFs can be endowed with real-time imaging capability, while the incorporation of photothermal or photodynamic agents enhances therapeutic potency through synergistic phototherapy. Furthermore, hybrid architectures that merge COFs with nanomaterials such as magnetic or gold nanoparticles create multimodal carriers capable of MRI-guided therapy, hyperthermia activation, and diagnostic imaging. A notable example is the development of a COF–SPION (superparamagnetic iron oxide nanoparticle) theranostic nanoplatform, which exemplifies the feasibility of integrating therapeutic and diagnostic functionalities into a single COF-based system.[58]

3. Covalent organic frameworks (COFs)

3.1 Linkages in COFs: chemistry, stability, and biomedical relevance

The structural and functional diversity of COFs is fundamentally rooted in the chemistry of their linkages. These covalent bonds between organic building units dictate not only the overall crystallinity and porosity of the framework, but also its mechanical robustness, hydrolytic stability, and compatibility with biological environments—properties that are decisive in drug delivery applications. Over the past two decades, advances in synthetic methodology have progressively expanded the library of linkages, enabling frameworks with tunable stabilities, chemical reactivities, and responsiveness to stimuli. The evolution of these linkages can be traced back to the seminal contributions of Yaghi and co-workers, who first demonstrated the potential of boroxine- and boronate ester-linked 2D COFs in 2005,[38] followed shortly thereafter by the introduction of their 3D counterparts.[59] These pioneering studies laid the foundation for the modular construction of extended porous architectures, though the inherent hydrolytic lability of boron–oxygen linkages posed limitations for biological use.

To overcome these challenges, attention shifted to more robust linkages such as imines and β-ketoenamines. Imine-linked COFs, exemplified by the synthesis of COF-300 in 2009,[60] quickly became popular due to their relatively straightforward synthesis *via* Schiff-base condensation and their moderate chemical stability. However, imine bonds are susceptible to hydrolysis under acidic or physiological conditions, which can restrict their application *in vivo*. The emergence of β-ketoenamine linkages marked a transformative advance in COF chemistry, setting a new standard for hydrolytic resilience. A transformative advance came in 2012, when Banerjee and co-workers reported the first β-ketoenamine-linked COFs.[61] The synthesis proceeded through a two-step process: an initial reversible Schiff-base reaction produced an ordered imine-linked framework, which subsequently underwent irreversible enol-to-keto tautomerization. This tautomerization effectively ''locked'' the framework into the chemically inert β-ketoenamine form without disrupting crystallinity, since only bond rearrangements occur while atomic positions remain nearly unchanged. The resulting materials exhibited unprecedented stability among COFs at the time—TpPa-1 resisted degradation in boiling water and strong acid, while TpPa-2 demonstrated additional resistance to concentrated base. This pioneering work firmly established β-ketoenamine linkages as a benchmark in COF chemistry by showing that crystallinity and extraordinary chemical resilience could be achieved simultaneously. Such durability is particularly valuable for drug delivery, where frameworks must maintain their structural integrity and porosity in aqueous and physiological environments to ensure predictable loading and sustained release performance.

Hydrazone-linked COFs represent another versatile class, notable for their dynamic covalent chemistry and their intrinsic pH-responsiveness. First introduced in frameworks such as COF-42 and COF-43,[62] hydrazone linkages have been widely utilized for conjugating drugs to polymeric carriers, exploiting their accelerated hydrolytic cleavage at acidic pH.[63] This property is particularly attractive for cancer therapy, where the acidic tumor microenvironment can trigger localized drug release, minimizing systemic toxicity. Beyond imine derivatives, triazine linkages emerged as an early strategy to enhance COF stability. Synthesized *via* trimerization of dicyanobenzenes under ionothermal conditions, triazine frameworks exhibit exceptional chemical and thermal resilience due to their aromatic, nitrogen-rich backbones.[64] Their robustness makes them suitable for harsh catalytic conditions, and in a biomedical context, their nitrogen sites offer opportunities for hydrogen bonding and guest stabilization. Polyimide linkages extended this trend by endowing frameworks with exceptional acid/base stability and large mesopores (up to 53 Å),[65] offering the potential to accommodate macromolecular drugs or biological cargos that would be inaccessible to smaller-pore COFs.

Several other linkage chemistries have progressively enriched the structural landscape of COFs. Phenazine-linked COFs, synthesized by Jiang and colleagues in 2013,[66] demonstrated impressive nitrogen adsorption and high surface areas, highlighting the role of extended π-conjugation in stabilizing the framework while promoting electronic conductivity. Urea linkages, introduced by Yaghi *et al.* in 2018,[67] brought directional hydrogen bonding motifs into COFs, providing an avenue to stabilize encapsulated biomolecules *via* noncovalent interactions. Similarly, amide linkages, initially accessed *via* post-synthetic oxidation of imines[68] and later through direct ester–amine exchange reactions,[69] have proven exceptionally resilient under physiological conditions, rivaling the stability of peptide backbones.

The expansion of COF chemistry into less conventional linkages has also introduced materials with unique functional properties. Olefin-linked COFs[70] display remarkable water stability and conjugated π-backbones that facilitate charge transport, which could be harnessed for phototherapy-enhanced drug delivery. Dioxin-linked COFs[71,72] introduced highly stable aromatic ether linkages, while phosphazene-linked frameworks[73] brought new opportunities for biocompatibility through their unique P–N backbones. The recent development of nitrone-linked COFs (COF-115)[74] further diversified the chemical space, demonstrating water harvesting and gas adsorption potential while being photo-convertible into amide-linked frameworks. Most recently, polyphenylene COFs synthesized *via* aldol cyclotrimerization[75] underscored the continued expansion of linkage chemistry into conjugated, hydrolytically stable domains, thereby reinforcing the promise of COFs in bioelectronics-integrated drug delivery.

From a biomedical perspective, the selection of linkage chemistry is not only a structural consideration but also a determinant of functional performance. Hydrolytically labile linkages such as hydrazones enable stimuli-responsive release, while resilient linkages such as β-ketoenamines, polyimides, and amides provide stability under physiological conditions, ensuring that drug carriers remain intact until reaching their biological targets. In addition, the polarity and hydrogen-bonding characteristics imparted by specific linkages modulate drug–framework interactions, influencing encapsulation efficiency, solubility, and release kinetics. Post-synthetic modification of linkages offers further control, permitting functionalization with targeting ligands or PEG chains[76] to enhance circulation times and tumor specificity. The chemical ingenuity behind COF linkages has steadily expanded the toolbox for designing biomedically relevant frameworks. Each linkage type embodies a balance between synthetic accessibility, chemical stability, and functional tunability, enabling tailored frameworks for precision drug delivery. Fig. 2 traces this chronological evolution, illustrating how innovations in linkage chemistry have progressively broadened the scope of COFs from fragile boron-based networks to chemically resilient, multifunctional nanocarriers with direct biomedical utility.

3.2 Synthesis methodologies for COFs

The synthesis of COFs elegantly hinges on the delicate interplay between kinetic control—which initiates network formation—and thermodynamic control—which guides the system to crystallinity through reversible bond formation. Unlike coordination polymers or supramolecular assemblies, COFs are constructed from robust covalent bonds (bond dissociation energies: 50–110 kcal mol^{-1}), which are less dynamic and more difficult to reversibly reorganize.[30] Achieving crystallinity thus requires conditions that promote error correction—that is, the capacity for bonds to break and reform until the system converges toward the thermodynamically most stable crystalline product. If the assembly proceeds too quickly, kinetic products—amorphous or poorly ordered polymers—dominate. If reversibility is too low, structural defects such as dangling bonds or misaligned linkages persist. Therefore, the reaction environment must encourage reversible bond exchange (dynamic covalent chemistry), allowing the network to "self-heal" by eliminating energetically unfavorable arrangements during crystal growth. At ambient conditions, these processes are often hindered by high activation barriers for covalent bond rearrangements, making ordered COF formation challenging. To overcome this limitation, a spectrum of synthetic protocols has been developed, each tailored to manipulate reaction kinetics and thermodynamics in distinct ways. These approaches vary not only in terms of operational parameters (temperature, solvent, pressure) but also in their scalability, environmental footprint, and compatibility with specific linkages and morphologies (bulk powders, films, single crystals). Below we summarize the major methodologies, emphasizing

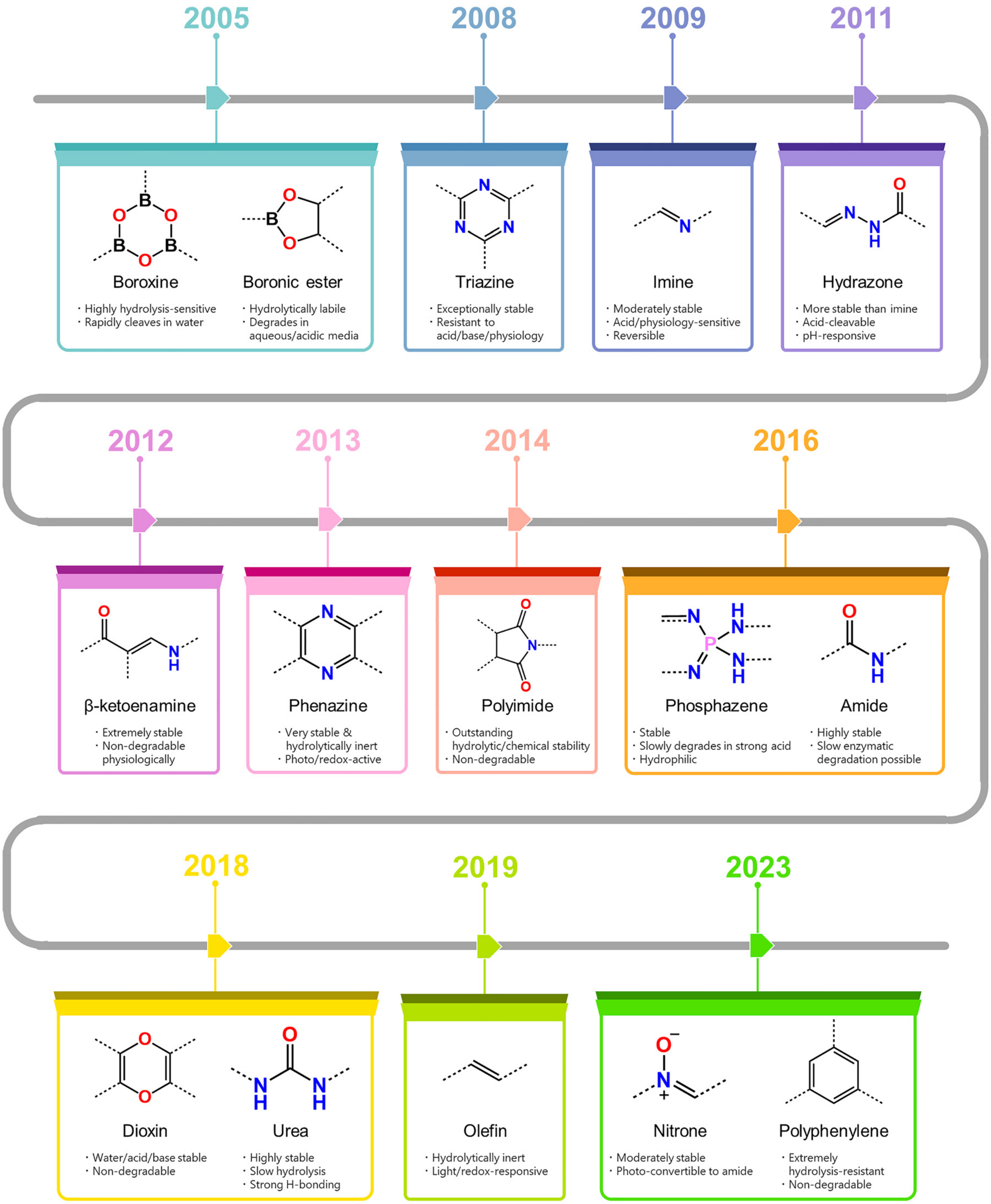

Fig. 2 Timeline of COF linkage innovations highlighting chemical stability, hydrolytic sensitivity, degradability, and stimuli-responsiveness.

their mechanistic underpinnings, unique advantages, and current limitations.

3.2.1 Solvothermal synthesis. Solvothermal synthesis remains the archetypal and most widely employed route to COFs. It typically involves sealed reaction vessels (*e.g.*, Pyrex tubes) charged with monomers, sometimes combined with modulators and acid catalysts, then heated (typically between 80–200 °C) for extended periods (1–7 days). The sealed environment enables autogenous pressure and high local supersaturation, which facilitate reversible bond exchange and promote long-range ordering. A critical feature of solvothermal synthesis is the careful tuning of the solvent system. Binary solvent mixtures (*e.g.*, mesitylene/dioxane, mesitylene/DMF) are often employed to modulate solubility and polarity, thereby controlling nucleation and growth rates. Catalysts such as acetic acid or *p*-toluenesulfonic acid enhance bond reversibility, while modulators (*e.g.*, aniline) can slow down nucleation and improve crystallinity. This methodology was pioneered by

Yaghi and co-workers in 2005, who synthesized COF-1 (based on boronic ester linkages) and COF-5, revealing two-dimensional networks with impressive porosity and crystallinity *via* solvothermal conditions.[38] The hallmark advantage of solvothermal synthesis is its broad versatility: nearly all classical COF linkages—including boronate esters, imines, hydrazones, and β-ketoenamines—were first realized *via* this approach. Moreover, it produces COFs with relatively high crystallinity and porosity. However, it is not without drawbacks. Solvothermal methods are typically time-intensive, require careful optimization through trial-and-error, and often involve toxic organic solvents. Furthermore, scaling up these reactions is challenging because homogeneous heating and solvent sealing become impractical at larger volumes.

3.2.2 **Microwave-assisted synthesis.** Microwave heating has emerged as an attractive alternative to traditional solvothermal methods. By coupling electromagnetic energy directly into the reaction medium, microwaves induce rapid and uniform volumetric heating, dramatically accelerating bond exchange and crystallization. Reaction times are reduced from several days to minutes or hours, and product yields are generally higher due to more homogeneous nucleation conditions. Microwave-assisted synthesis is particularly well-suited to imine- and boronate ester-linked COFs, where bond reversibility is sufficient to allow for rapid error correction under short bursts of energy input. Li *et al.* exemplified this with the imine-linked Mw-TFB-BD-X COFs synthesized under air in just one hour, exhibiting both enhanced crystallinity and superior iodine adsorption performance compared to their solvothermal counterparts.[77] Another striking example is COF-5, synthesized *via* microwave irradiation in just 20 minutes at 100 °C, yielding exceptionally high surface area comparable to traditional methods.[78] Notably, water-assisted microwave protocols have also been developed, offering greener conditions while maintaining crystallinity.[79] The principal advantages of this method are speed, energy efficiency, and scalability. However, it requires specialized equipment, and the fast heating ramps may sometimes promote kinetic trapping if not carefully controlled. Additionally, COFs with sluggish reversible chemistry (*e.g.*, amides, imides) may require optimization to prevent incomplete crystallization.

3.2.3 **Mechanochemical synthesis.** Mechanochemical synthesis exploits mechanical energy—*via* manual grinding or automated ball milling—to drive bond formation at room temperature, often with minimal or no solvent. This approach reduces reliance on toxic organic solvents, shortens reaction times, and aligns with the principles of green chemistry. Early studies demonstrated the solvent-free preparation of β-ketoenamine-linked COFs by simple grinding of monomers in a mortar.[80] More recently, liquid-assisted grinding (LAG) has been used to accelerate reversibility and improve crystallinity by adding a few drops of liquid that act as a transient reaction medium.[81] Acidic additives such as *p*-toluenesulfonic acid can further promote dynamic bond exchange, enabling ordered frameworks.[82] Mechanochemistry offers several unique advantages: it is environmentally benign, energy-efficient, and scalable. Ball milling, in particular, can generate crystalline COFs within minutes and has enabled the synthesis of functional COFs for gas capture and separations.[83] The main limitation lies in crystallinity, which is often lower than that obtained by solvothermal methods, and the method is less general for linkages that require high-temperature activation. Nevertheless, recent developments in *in situ* monitoring (XRD, Raman) have shed light on mechanistic pathways, paving the way for rational mechanochemical design.[84]

3.2.4 **Ionothermal synthesis.** Ionothermal methods replace traditional organic solvents with molten salts or ionic liquids (ILs). These reaction media possess unique physicochemical properties—high polarity, negligible vapor pressure, and strong Lewis acidity—that enable COF formation under unconventional conditions. A prototypical example is the synthesis of covalent triazine frameworks (CTFs) using molten $ZnCl_2$ at $\sim$400 °C, where $ZnCl_2$ serves both as solvent and catalyst, promoting nitrile trimerization into triazine rings.[85] Lotsch and co-workers further expanded the scope of ionothermal synthesis by developing a $ZnCl_2$-mediated route to imide-linked COFs, enabling rapid ($\sim$10 h) and scalable formation of crystalline frameworks under solvent- and catalyst-free conditions, while also demonstrating that the use of eutectic salt mixtures can lower reaction temperatures and broaden compatibility to less stable linkers.[86] In parallel, ILs such as [BMI][NTf_2] have been employed to direct the formation of 3D COFs, enabling significantly accelerated synthesis—ranging from just three minutes for 3D-IL-COF-1 to 12 hours for 3D-IL-COF-2 and 3D-IL-COF-3—compared to the conventional timescales of several days.[87] Ionothermal synthesis enables access to frameworks with exceptional chemical and thermal stability that are difficult to obtain *via* solvothermal conditions. The advantages include solvent-free processing, shorter reaction times, and the ability to synthesize COFs with high stability and crystallinity. However, high temperatures and corrosive salts can limit the range of compatible linkers and make post-synthetic purification challenging. Scalability is promising, but energy costs must be carefully weighed.

3.2.5 **Interfacial polymerization.** Interfacial polymerization (IP) provides a powerful strategy for constructing COFs as thin films or membranes. By confining monomers at the interface between immiscible solvents (*e.g.*, aqueous and organic phases), COF growth is restricted to two dimensions, allowing precise thickness control and enabling direct film transfer onto substrates. The advantages of IP are particularly notable in membrane science: COF films produced in this manner are defect-free, continuous, and transferable to supports while retaining crystallinity and porosity.[88] Moreover, the film thickness can be tuned from nanometers to micrometers, which is critical for optimizing flux and selectivity in separations. Despite these strengths, challenges remain. Aggressive solvents are often required, limiting compatibility with polymeric supports. Reaction times can be long, and adhesion of COF films to substrates may be poor. Nonetheless, innovations such as salt-mediated IP[89] and direct polymer-substrate growth[90] have substantially improved film quality and scalability.

3.2.6 Ambient-condition synthesis. A growing body of work has demonstrated the possibility of synthesizing crystalline COFs under ambient conditions—room temperature and atmospheric pressure—by leveraging monomer solubility and strong noncovalent interactions such as π–π stacking. Remarkably, COFs synthesized at room temperature often exhibit crystallinity and porosity comparable to their solvothermal counterparts. This approach is particularly advantageous for fragile linkers that would otherwise decompose at elevated temperatures. Moreover, continuous-flow setups have demonstrated high-throughput production with excellent space-time yields, underscoring industrial potential.[91] Vapor-assisted conversion[92] and even gamma irradiation[93] protocols have further expanded the scope of ambient-condition synthesis, allowing controlled thin-film growth or rapid crystallization in air. The key advantages are simplicity, energy savings, and compatibility with sensitive monomers. The main drawback is the limited generality: many linkages still require high temperatures to achieve sufficient reversibility for crystalline ordering.

3.2.7 Sonochemical synthesis. Sonochemistry harnesses acoustic cavitation—rapid bubble formation and collapse under ultrasonic irradiation—to generate localized microenvironments of extreme temperature (>5000 K) and pressure (>1000 bar).[94,95] These transient "hot spots" accelerate bond formation and enhance nucleation, enabling the synthesis of crystalline COFs within minutes to hours. Sonochemical methods are inherently energy-efficient, as no induction period is needed and crystallization is significantly faster than under solvothermal conditions. They have been particularly useful for high-throughput synthesis of COFs and conjugated polymers for photocatalysis.[96] The advantages are rapid reaction rates, low energy consumption, and scalability for screening libraries of COFs. However, control over particle morphology and size can be challenging, and mechanistic understanding of cavitation-driven bond exchange remains incomplete.

3.2.8 Single-crystal COF synthesis. Perhaps the most formidable challenge in COF chemistry is the growth of single crystals large enough for unambiguous structural determination by X-ray diffraction. Most COFs have historically been characterized by powder diffraction and modeling, leading to uncertainties in stacking arrangements, topology, and subtle structural details. Recent advances have demonstrated that careful modulation of reversibility is the key to single-crystal growth. Initial efforts by Yaghi and co-workers employed aniline as a modulator to slow growth and facilitate single-crystal formation of imine-linked COFs, producing crystals up to 100 μm in 15–80 days.[97] Subsequently, Wang and colleagues dramatically accelerated single-crystal formation by using trifluoroacetic acid (CF_3COOH) as a catalyst and trifluoroethylamine ($CF_3CH_2NH_2$) as a modulator, achieving well-defined single crystals (50–150 μm) in just 1–2 days, with sub-Å resolution.[98] Other strategies include combining dynamic covalent chemistry with labile metal coordination to form metallo-COFs,[99] employing a two-step seeded growth procedure where monomers are added slowly to preformed nanoparticles,[100] and exploiting single-crystal-to-single-crystal transformations *via* redox conversion of imine linkages into amine and amide ones.[101] Single-crystal COFs unlock unprecedented opportunities: direct visualization of stacking disorder,[102] identification of growth intermediates,[103] and atomic-level resolution of guest–host interactions.[104] Nevertheless, the synthesis remains highly challenging, time-intensive, and often limited to a small subset of linkages. Machine-learning (ML)-guided optimization of crystallization landscapes represents an exciting new direction to overcome these limitations.

The key approaches to COF synthesis, along with their essential features, strengths, and constraints, are outlined in Table 1.

3.3 Applications of green-synthesized COFs in drug delivery

To meet the twin goals of clinical safety and environmental sustainability, COF synthesis for drug-delivery applications must move beyond proof-of-concept chemistry and adopt green, life-cycle-aware manufacturing practices while explicitly assessing how those choices alter carrier performance (drug loading, release, stability, and *in vivo* fate). Below we outline three actionable strategies—solvent greening, catalyst recovery/reuse, and degradable-linker design—and summarize what evidence exists today and what evaluation metrics should be reported when claiming a "green" COF for nanomedicine.

3.3.1 Solvent greening: replace toxic high-boiling solvents with water/alcohol-based routes and quantify performance trade-offs. Recent methods (alcohol-assisted hydrothermal polymerization, ambient aqueous/ionothermal, and microwave-assisted approaches) demonstrate that many stable COF linkages can be formed with little or no reliance on classical high-boiling toxic mixtures (*e.g.*, mesitylene/dioxane), reducing solvent consumption by ≈70–90% in some reports. These greener routes often give comparable crystallinity and porosity to solvothermal products, and it is increasingly important for studies to quantify both the environmental benefits and the functional performance of the resulting materials. This includes reporting green metrics—such as the reduction in solvent volume and hazard relative to conventional solvothermal conditions—together with key structural and application-relevant parameters (*e.g.*, BET surface area, PXRD-derived crystallinity, and drug loading/release profiles obtained under identical experimental conditions) to enable transparent assessment of any performance–sustainability trade-offs. Notably, alcohol-assisted hydrothermal polymerization (aaHTP) of imide COFs has demonstrated toxic solvent reductions approaching ∼90% while still producing materials with high porosity and crystallinity comparable to traditional methods.[105] Ambient aqueous and microwave-assisted syntheses further speed production and reduce energy/solvent footprints.[106]

From a practical standpoint, transparent comparison requires that each green synthesis route be accompanied by clear reporting of (a) solvent usage and associated hazard indices relative to a solvothermal reference, (b) drug-loading data obtained using strictly matched conditions (identical drug concentration, incubation time, solvent environment, and

Table 1 Overview of COF synthesis strategies with associated features, strengths, and shortcomings

Methods	Key features	Advantages	Limitations
Solvothermal	Thermal control of reversibility	• High crystallinity and porosity • Broad applicability across linkages	• Long reaction times • Trial-and-error optimization • Uses toxic or high-boiling solvents • Scaling is complex due to heat and pressure management
Microwave-assisted	Rapid volumetric heating	• Ultra-fast • Efficient • Greener	• Requires specialized microwave reactors • Fast heating may risk kinetic trapping if bond reversibility is inadequate • Not universally effective for all linkage chemistries
Mechanochemical	Mechanical energy-driven, often solvent-free	• Solvent-free or minimal solvent—greener approach • Fast and scalable • Mild	• Often lower crystallinity and reduced surface area compared to solvothermal methods • Limited to linkage types with accessible reversibility under mechanical energy
Ionothermal	Ionic liquid/molten salt medium	• Produces COFs with high thermal/chemical stability • Often faster than solvothermal equivalents • Scalable potential, especially with eutectic mixtures to lower reaction temperatures	• High-temperature requirement may limit fragile linkers • Post-synthetic removal of ionic media can be challenging • Cost and corrosiveness of salts/ionic liquids may hinder scalability
Interfacial polymerization	2D film growth at fluid interfaces	• Thin COF films with precise thickness control • High crystallinity and porosity retained in membrane format • Direct transfer to substrates (glass, metal, grids) • Enhanced permeability and selectivity in separations	• Often requires harsh solvents and long reaction times • Adhesion issues and substrate compatibility • Process complexity in film transfer
Ambient-condition	Mild, nonthermal activation	• Mild conditions suitable for sensitive monomers • Energy-efficient and safe • Compatible with continuous-flow formats • Vapor-assisted film synthesis enables thickness tuning and large-area coverage • Gamma irradiation under ambient air promotes crystallization across opaque vessels	• Applicability limited to monomers with sufficient noncovalent stabilizing interactions • Generality to broader COF types still under development
Sonochemical	Cavitation-induced micro-hotspots	• Exceptionally fast reactions without incubation periods • Energy-efficient • Easily scalable	• Limited control over particle size/morphology • Mechanistic pathways of cavitation-driven crystallization remain under investigation
Single-crystal	Slow, modulated crystal growth	• Atomic-level insight into topology, stacking, guest interactions, and dynamics • Supports mechanistic studies *via* detection of intermediates and stacking evolution • Enables studies of crystal dynamics and stability	• Extremely time-consuming (days to weeks) • Limited to a narrow range of linkages and conditions

temperature), and (c) corresponding *in vitro* release profiles measured under the same protocol. Existing side-by-side evaluations indicate that hydrothermal or aqueous COFs often exhibit drug-loading efficiencies within a few weight percent of their solvothermal counterparts, although such assessments are only meaningful when all loading and release parameters are rigorously controlled.

3.3.2 Catalyst recovery and recycling: use recyclable acidic ILs or heterogeneous acid catalysts and quantify residual catalyst risk. Acidic ILs and task-specific ILs have emerged as effective, recyclable catalysts for many condensation reactions. For green COF manufacture, ILs offer two advantages: they can catalyse condensation at lower temperatures or in greener solvent mixes, and they can often be recovered and reused by simple phase separation or evaporation, lowering both cost and catalyst residue in the product. When ILs are used, studies should report (a) catalyst turnover number (TON) and reuse cycles with retained COF quality (PXRD/BET), (b) quantitative catalyst leaching/residual analysis (*e.g.*, by NMR, ion chromatography or ICP-MS when metalated ILs are used), and (c) cytotoxicity assays of residual catalyst and the purified COF to ensure biosafety.

Key quantitative indicators that enable meaningful assessment of IL-based COF synthesis include the percentage of IL recovered per batch, retention of COF structural quality (*e.g.*, PXRD patterns and BET surface areas) after multiple catalyst-reuse cycles, the concentration of residual IL in the purified COF (typically reported in ppm), and the cytotoxicity profiles of COF wash fractions generated during purification.

3.3.3 Biodegradation-by-design: incorporate hydrolysable or stimulus-cleavable linkers so COFs are cleared after therapeutic action. A compelling green-nanomedicine strategy is to design COFs that perform their delivery role and then degrade into small, excretable fragments. Recent studies demonstrate several viable approaches: redox-cleavable (disulfide) linkers that degrade in the tumor-selective reducing environment (GSH-rich), acid-labile ester or β-amino-ester linkers responsive to endosomal/tumor pH, and azo or other ROS-cleavable motifs activated in tumor microenvironments. These systems show accelerated drug release in the intended microenvironment and improved biosafety profiles because the breakdown products are low-molecular-weight organics readily handled by renal/hepatic clearance. Representative experimental examples include disulfide-linked porphyrin COFs that undergo GSH-triggered nanocrystallization and degradation with demonstrated tumor-selective drug release and acceptable organ histology.[107]

Essential characterization parameters for degradable COFs include: (a) the chemical identity and biological fate of degradation products, typically determined by LC–MS and NMR; (b) quantitative *in vitro* degradation kinetics under physiologically relevant conditions—such as PBS (pH 7.4), mildly acidic environments (pH ∼ 5.5), or glutathione-rich media (10 mM GSH)—with half-lives expressed on an hourly timescale; (c) *in vivo* degradation and excretion profiles obtained through urine, feces, bile, and organ-residue analyses; and (d) comprehensive evaluation of systemic toxicity and immunogenicity associated with both the intact COF and its breakdown fragments. Existing degradable COF platforms consistently demonstrate rapid, stimulus-responsive degradation and tumor-selective drug release. To enable rigorous safety assessment, studies should quantify the extent of mass loss over defined time intervals (*e.g.*, percentage degraded within 24–72 hours) and precisely identify the resulting fragments so that clearance mechanisms and potential toxicities can be fully evaluated.

4. COFs as carriers for precision and controlled drug delivery

4.1 Introduction to COFs as drug carriers

COFs have increasingly distinguished themselves as promising nanocarriers for therapeutic applications. Unlike many inorganic or metal–organic carriers, COFs are composed solely of light elements (C, N, O, B, *etc.*), eliminating concerns of heavy-metal cytotoxicity while simultaneously reducing carrier weight and enhancing drug-to-carrier ratios. Their crystalline, permanently porous architectures, along with modular tunability, make them particularly attractive for precision nanomedicine, where pore size, geometry, and surface chemistry can be deliberately tailored to regulate drug loading, release kinetics, and cellular targeting.

The first experimental demonstration of COFs for controlled drug delivery was provided by Fang and co-workers in 2015.[108] They reported the synthesis of two 3D polyimide-linked COFs (PI-COF-4 and PI-COF-5), generated by condensing tetrahedral building blocks with pyromellitic dianhydride through imidization. The resulting frameworks presented narrow yet well-defined pore apertures (13 Å for PI-COF-4 and 10 Å for PI-COF-5), providing a structurally precise host environment for encapsulation of ibuprofen, a small-molecule NSAID with a short half-life. Drug release profiles were monitored *via* UV-vis spectrophotometry, where the calibration curve of ibuprofen absorption confirmed accurate quantification of release kinetics (Fig. 3a). Importantly, this study demonstrated a direct correlation between pore geometry and drug-release behavior: the non-interpenetrated PI-COF-4 with larger pore size enabled faster ibuprofen release compared to the 4-fold interpenetrated PI-COF-5 with smaller pore size. Over the course of seven days, both COFs achieved nearly complete release (∼95%) (Fig. 3b), underscoring their potential as sustained-release formulations. Conceptually, this was the first evidence that COF topology is not merely a crystallographic curiosity, but an active determinant of PK performance.

Building upon this principle, Zhao and colleagues in 2016 reported imine-linked COFs, PI-2-COF and PI-3-COF, with microporous structures and pore dimensions of 1.4 and 1.1 nm, respectively.[109] Here, the authors extended the drug panel to ibuprofen, captopril, and 5-fluorouracil (5-FU), thereby providing a broader proof of concept. The larger-pore PI-2-COF exhibited drug loading up to 30 wt%, significantly surpassing prior frameworks. Biological assays revealed that both COFs were biocompatible (cell viability > 80% even at 200 μg mL^{-1}), but their drug-loaded analogues displayed dose-dependent cytotoxicity in cancer cell lines. Notably, 5-FU-loaded COFs significantly inhibited MCF-7 breast cancer cells, with the more porous PI-2-COF showing stronger efficacy due to its superior loading. Fluorescence microscopy confirmed cellular uptake of COFs *via* endocytosis, directly establishing the feasibility of COFs as intracellular drug carriers. This work emphasized structure–function relationships in pore size and geometry, and importantly, provided early evidence that COFs could act as safe and effective intracellular vehicles for chemotherapy agents.

4.2 Molecular recognition and non-covalent host–guest interactions in COF drug delivery

Beyond pore confinement and size exclusion, molecular recognition governed by non-covalent host–guest interactions has emerged as a decisive factor in controlling drug loading efficiency, retention stability, and release behavior in COF-based nanocarriers. The ordered π-conjugated backbones and chemically addressable pore surfaces of COFs provide a unique platform in which π–π stacking, hydrogen bonding, electrostatic

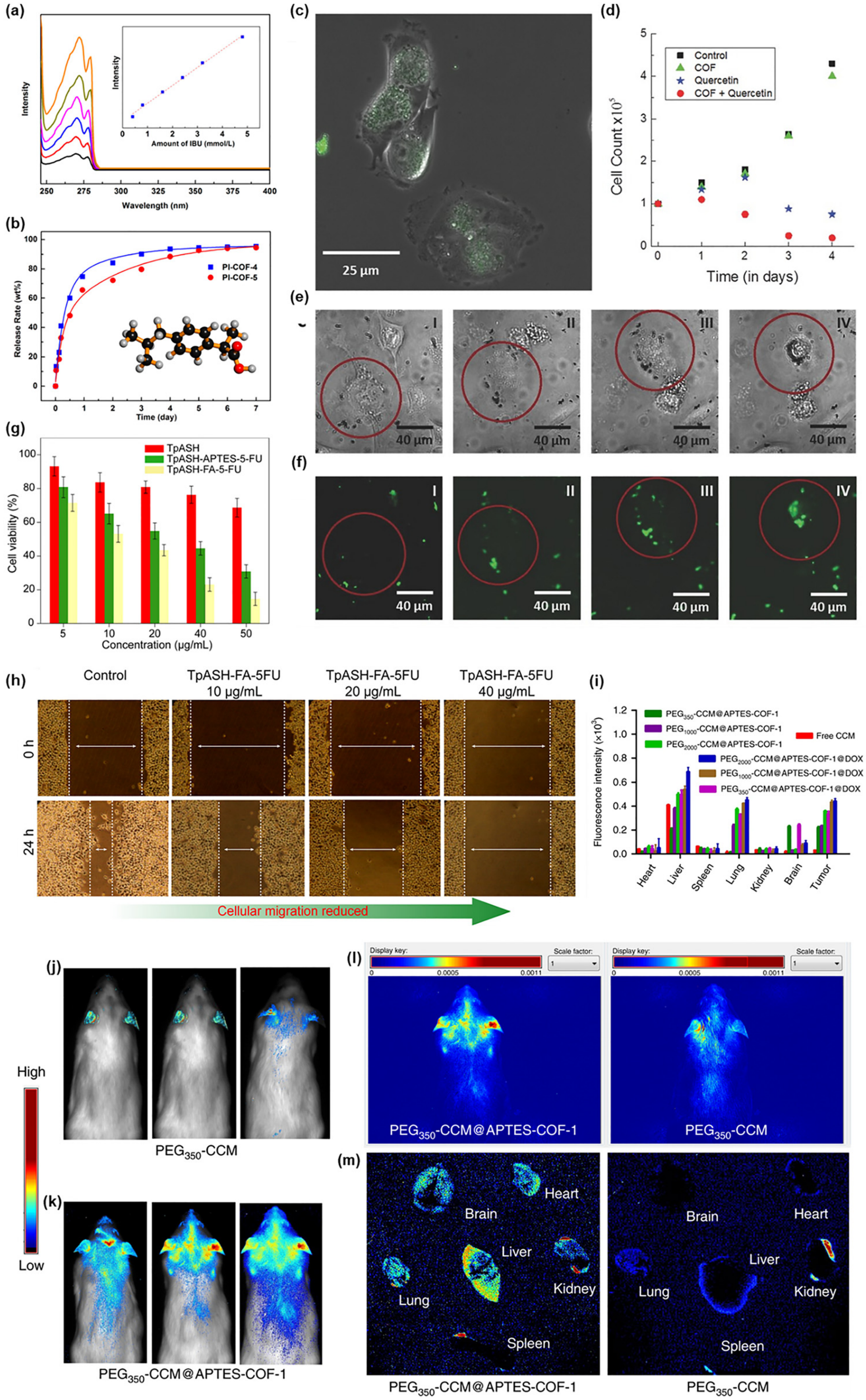

Fig. 3 (a) UV-vis absorption spectra of ibuprofen in simulated body fluid (pH 7.4) at varying concentrations with calibration curve (inset). (b) Ibuprofen release from 3D PI-COFs and structural representation of ibuprofen (inset). Adapted with permission from ref. 108. Copyright 2015 American Chemical Society. (c) Merged fluorescence and phase-contrast micrograph depicting efficient COF internalization in MDA-MB-231 cells. (d) Time-dependent cell proliferation assay showing responses to COF, Quercetin, and Quercetin-loaded COF compared to untreated controls. (e) and (f) Time-lapse phase-contrast (e) and fluorescence (f) microscopy images revealing Quercetin-loaded COF uptake and apoptosis. Adapted with permission from ref. 110. Copyright 2016 Wiley-VCH Verlag GmbH & Co. KGaA, Weinheim. (g) MTT assay demonstrating enhanced anticancer efficacy of targeted CONs (TpASH-FA-5-FU) relative to non-targeted analogues. (h) Migration assays of cells treated with TpASH-FA-5-FU compared to control. Adapted with permission from ref. 47. Copyright 2017 American Chemical Society. (i) Quantified fluorescence intensity of CCM across organs and tumor measured 24 h after injection. (j) and (k) Brain imaging confirms uptake following injection with PEG350-CCM or PEG350-CCM@APTES-COF-1. (l) Visualization of tumor localization and systemic biodistribution. (m) *Ex vivo* fluorescence assessment of vital organs. Adapted with permission from ref. 111. Copyright 2018, The Author(s).

interactions, and van der Waals forces can be deliberately exploited to enhance drug–framework affinity at the molecular level. A seminal contribution in this direction was reported by Lotsch and co-workers, who employed an imine-linked COF as a functional host for quercetin, a polyphenolic flavonoid with intrinsic anticancer activity.[110] In this study, solid-state NMR spectroscopy provided direct evidence for hydrogen-bonding interactions between the imine nitrogen atoms of the COF and the hydroxyl groups of quercetin, which stabilized encapsulation and suppressed premature drug leakage. To probe biological relevance, *in vitro* studies with human MDA-MB-231 breast carcinoma cells were carried out. Fluorescence microscopy images acquired two hours after introducing the COF into the culture medium revealed clear internalization of the particles by the cancer cells (Fig. 3c). When the Quercetin-loaded COF was added, time-lapse imaging further demonstrated COF nanoparticle uptake accompanied by marked apoptotic responses in the treated cells (Fig. 3e and f). Complementary cell-proliferation assays showed that the pristine COF itself was largely biocompatible, with cell counts increasing comparably to untreated controls, whereas Quercetin-loaded COFs significantly suppressed proliferation (Fig. 3d). These findings directly linked COF-mediated drug delivery with therapeutic outcomes and highlighted molecular-level host–guest recognition as a powerful design handle for nanocarriers, moving beyond simple size-exclusion or pore confinement effects. More recently, conjugation-driven host–guest chemistry has been explicitly demonstrated as a governing principle for selective drug encapsulation. In a phenazine-linked π-conjugated COF (TU-32), it was shown that extended π-systems embedded within the COF backbone can selectively interact with conjugated drug molecules through π–π stacking, leading to markedly enhanced loading efficiencies.[50] Notably, TU-32 exhibited an atypical AB stacking mode, which suppressed interlayer π–π stacking between COF sheets while simultaneously improving pore accessibility and diffusion pathways. This structural feature decoupled framework crystallinity from guest binding, allowing in-pore π–π interactions between the conjugated COF walls and drug molecules to dominate the loading process. Comparative drug loading studies using 5-FU, isoniazid, and captopril revealed a clear correlation between molecular conjugation and loading efficiency. The fully conjugated heteroaromatic structure of 5-FU resulted in the highest loading capacity (56 wt%), followed closely by isoniazid (54 wt%), which contains a partially conjugated pyridyl moiety. In contrast, captopril—lacking an extended π-system—exhibited substantially lower loading (36 wt%). These results provide compelling experimental evidence that π–π stacking interactions, rather than pore size alone, can dominate guest affinity in π-engineered COFs. Moreover, sustained release profiles observed for conjugated drugs further indicate that such interactions contribute not only to high loading but also to enhanced retention and controlled release behavior. Taken together, these studies underscore a broader paradigm shift in COF-based drug delivery: from passive carriers relying primarily on geometric confinement to precision nanocarriers that leverage programmable molecular recognition. Hydrogen bonding, π–π stacking, and conjugation-matching between framework and guest molecules collectively enable selective encapsulation, improved stability, and tunable release kinetics. This emerging understanding provides a clear design blueprint for next-generation COF nanocarriers, where the electronic structure and functional chemistry of the framework are deliberately tailored to the molecular features of the therapeutic payload. Such conjugation- and interaction-guided strategies are expected to play an increasingly central role in the rational development of COFs for targeted and precision drug delivery applications.

4.3 Functionalization and targeting strategies

Banerjee and colleagues introduced yet another conceptual advance by marrying synthetic tunability with targeted therapy.[47] Using a salt-mediated synthesis route, they prepared two layered COFs (TpASH and TpAPH) and exfoliated them into covalent organic nanosheets (CONs). Through sequential postsynthetic modifications, TpASH was functionalized with folic acid (TpASH-FA), leveraging the overexpression of folate receptors on MDA-MB-231 breast cancer cells for selective targeting. Prior to drug loading, biocompatibility assays confirmed that the bare TpASH nanosheets were non-toxic, supporting their suitability as carriers. When loaded with the anticancer drug 5-FU, the targeted CONs demonstrated pronounced cytotoxicity toward the cancer cells, with only ∼14% cell viability at a dosage of 50 μg mL^{-1}, whereas nontargeted 5-FU-loaded CONs showed comparatively higher survival (Fig. 3g). In addition, cellular migration experiments revealed that treatment with the drug-loaded, folate-functionalized CONs substantially impeded the motility of MDA-MB-231 cells in a concentration-dependent manner, while untreated control cells exhibited normal migration patterns (Fig. 3h). The pH-responsive release of 5-FU, accelerated under acidic lysosomal conditions and sustained over 72 hours, combined with receptor-mediated uptake, underscores how modular postsynthetic chemistry in COFs can be harnessed to achieve selective, tumor-specific therapy—a capability that remains challenging with conventional carriers.

Jia and co-workers introduced a straightforward strategy to engineer water-dispersible nanocomposites by modifying APTES-COF-1 with polyethylene glycol–curcumin (PEG–CCM), thereby generating PEG–CCM@APTES-COF-1 assemblies that serve as intelligent nanocarriers for drug delivery.[111] The PEG functionalization acted as a PK regulator, markedly improving the colloidal stability, circulation lifetime, and biocompatibility of the COF-based system. Fluorescence imaging studies provided compelling evidence for the preferential tumor accumulation of these nanoassemblies. As shown in Fig. 3j and k, *in vivo* fluorescence imaging of brains collected from ICR mice at 4 h post injection revealed a much stronger signal at the tumor site for PEG_{350}–CCM@APTES-COF-1 compared to unassembled PEG_{350}–CCM, confirming the effective targeting and delivery capability of the COF nanoplatform. This trend is further highlighted in Fig. 3l, where the intensity contrast demonstrates the enhanced tumor localization of the COF nanoassemblies relative to free PEG–CCM. The *ex vivo* organ distribution profiles (Fig. 3m) corroborated these findings, indicating selective accumulation in tumor tissue with reduced nonspecific distribution to other organs. Cellular uptake experiments further revealed that the nanoassemblies were readily internalized by tumor cells, and the acidic microenvironment triggered the gradual disintegration of the COF scaffold, thereby ensuring efficient intracellular release of the encapsulated drug. When loaded with DOX, the PEG–CCM@APTES-COF-1@DOX system exhibited markedly deeper penetration, longer retention, and enhanced therapeutic performance compared to both free DOX and the non-PEGylated APTES-COF-1@DOX. This was particularly evident in Fig. 3i, where tumor-site fluorescence was significantly higher in PEG_{2000}–CCM@APTES-COF-1@DOX-treated mice than in those treated with free CCM or other formulations. The *in vivo* antitumor assays further validated the superiority of the PEG_{2000}–CCM@APTES-COF-1@DOX system, which achieved greater tumor suppression efficiency relative to free DOX and alternative PEG–CCM@APTES-COF-1@DOX formulations. These results demonstrated that PEG–CCM modification not only improves the PK behavior of COF-based carriers but also enables site-specific accumulation, pH-responsive release, and enhanced therapeutic efficacy against brain tumors.

4.4 Stimuli-responsive and smart COF nanocarriers

Recent work has further demonstrated the potential of COF nanocarriers to overcome prior limitations in cellular uptake and *in vivo* efficacy. In a 2024 study, a crystalline COF functionalized with long *n*-octyloxy side chains (TCPB–COF–C8) showed dramatically enhanced cellular internalization, bright red luminescence (λ_{em} = 632 nm, quantum yield 37%), and efficient loading and delivery of camptothecin (CPT). Upon systemic administration, this nanocarrier achieved ≈96% inhibition of tumor growth over 14 days, highlighting the feasibility of COF-based platforms for potent *in vivo* chemotherapy.[112] In a contribution from Lin *et al.*, DOX was *in situ* encapsulated into TAPB-DMTP-COF *via* a one-pot synthesis, which significantly shortened the drug-loading process while affording a relatively high loading efficiency.[113] The resultant DOX@COF exhibited excellent tumor inhibition *in vivo*, as evidenced by Fig. 4a and b, where the average relative tumor volume of the DOX@COF-treated group was markedly smaller than those of the PBS, COF, and free DOX groups, highlighting its enhanced anticancer efficacy. Zhang and co-workers reported PEGylated redox-responsive F68@SS-COFs that integrate an Pluronic F68 shell with disulfide-functionalized COFs, enabling substantial drug accommodation, durable stability in extracellular media, and favorable biocompatibility.[114] Fluorescence microscopy observations (Fig. 4c) revealed that DOX-loaded F68@SS-COFs enter tumor cells *via* endocytosis and rapidly release the drug in a GSH-rich environment, producing much stronger intracellular fluorescence than DOX-loaded F68@*n*-COFs. This work illustrates that PEGylation alongside disulfide incorporation can synergistically provide superior biocompatibility and precise intracellular release, ultimately boosting antitumor efficacy. Similar to their earlier F68@SS-COF design, the group further developed PEGylated CONs bearing hydrazone and disulfide bonds, which stably retained DOX under physiological conditions but rapidly disassembled in the acidic and reductive tumor microenvironment, ensuring efficient intracellular drug release.[49] By incorporating quinoline moieties, Li *et al.* achieved a COF-HQ with improved 5-FU loading and pH-dependent release behavior, ensuring enhanced drug accommodation and selective liberation of the payload in acidic environments.[115] Hemolysis testing (Fig. 4d) together with *in vivo* assays confirmed the excellent hemocompatibility and safety of the framework, while tumor models validated its superior therapeutic impact. A series of breakthroughs have shown how structural design and stimuli-responsiveness can dramatically expand the potential of COFs in drug delivery. Thioether-triazole TCOFs demonstrated dual sensitivity to acidic pH and glutathione, with PEGylated derivatives achieving stable dispersions and controlled doxorubicin release, underscoring the value of click-chemistry-derived flexibility.[116] Trabolsi and co-workers advanced the field further with nanoscale TTA-DFP-COFs as an oral insulin carrier, capable of protecting insulin under gastric conditions and achieving glucose-triggered pulsatile release (Fig. 4e and f), while preserving liver and kidney function *in vivo* (Fig. 4g).[117] Cage-based COFs offered another route to biocompatible, high-capacity nanocarriers,[118] and Jiang *et al.* pioneered hypoxia-responsive azo-linked COFs, where dual activation by oxygen depletion and NIR irradiation drove successive drug release and tirapazamine (TPZ) activation (Fig. 4h and i).[119] These studies demonstrated how smart chemistry and structural precision can transform COFs from passive carriers into adaptive nanoplatforms with spatiotemporally controlled release.

A wide range of innovative strategies have been reported to expand the biomedical scope of COFs by tailoring their structure, responsiveness, and function for advanced drug delivery. Tang *et al.* designed a COF-based smart theranostic nanosystem capable of both intracellular imaging and cancer-responsive chemotherapy (Fig. 5a).[120] By exploiting ssDNA as a gatekeeper, the system selectively released DOX in the acidic and biomarker-rich environment of cancer cells while remaining inert in normal cells. This selectivity was directly visualized by fluorescence imaging, where strong Cy5 and DOX signals were only observed in tumor cells (Fig. 5b). This work established a blueprint for COF–nucleic acid hybrid nanoplatforms in precision cancer therapy.

4.5 Topological and morphological engineering

Topology engineering has also emerged as a powerful handle to tune drug delivery behavior. Long *et al.* demonstrated that solvent- and concentration-controlled synthesis can selectively yield COFs with dual-pore (kagome) or single-pore (square) topologies.[121] The dual-pore architectures provided superior capacity for small-molecule drugs, underscoring the role of rational pore geometry in achieving controlled release. Moving from pore engineering to protein-mediated release, Bhattacharya *et al.* reported a perylene-based COF formulation

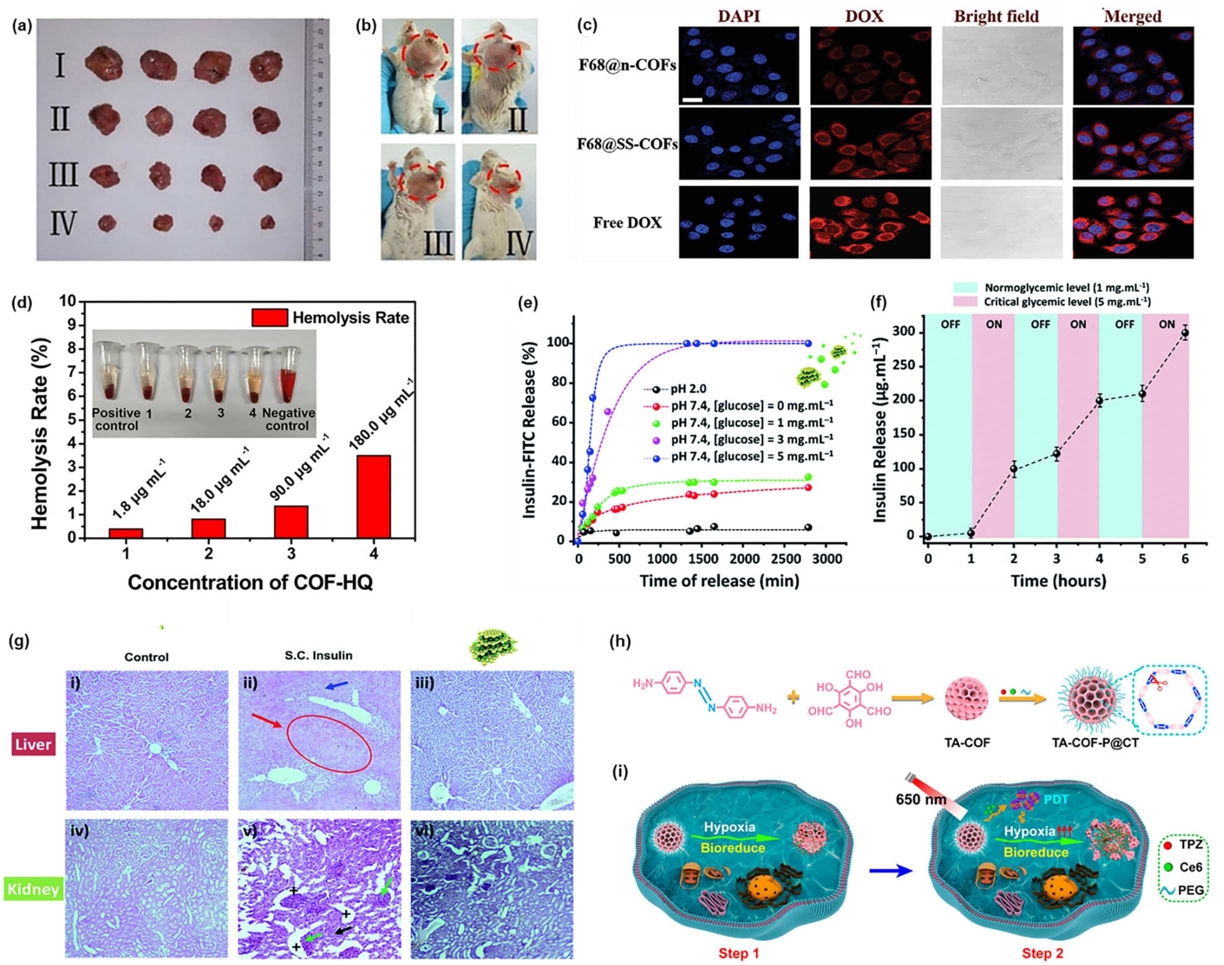

Fig. 4 (a) Tumor and (b) mouse photographs highlighting the superior anticancer performance of DOX@COF relative to control groups. Adapted with permission from ref. 113. Copyright 2019 Wiley-VCH Verlag GmbH & Co. KGaA, Weinheim. (c) Cellular uptake of DOX-loaded COFs visualized by fluorescence microscopy. Adapted with permission from ref. 114. Copyright 2020 Wiley-VCH Verlag GmbH & Co. KGaA, Weinheim. (d) Hemocompatibility analysis through hemolysis assay of COF-HQ at varying concentrations. Adapted with permission from ref. 115. Copyright 2020 Elsevier B.V. (e) and (f) Glucose/pH-responsive insulin release from TTA-DFP-nCOF. (g) Histopathological evaluation of liver and kidney tissues in control and treated diabetic rats. Adapted with permission from ref. 117. Copyright CC BY 3.0. (h) Synthesis of TA-COF-based therapeutic platforms. (i) Conceptual diagram of two-step light-driven hypoxia-responsive drug release. Adapted with permission from ref. 119. Copyright 2021, American Chemical Society.

stabilized with an albumin corona.[122] This platform achieved stimuli-driven drug release, where mitoxantrone (MXT) was discharged only upon albumin binding, ensuring spatiotemporal precision. Fig. 5c and d depict the design of the COF–protein system and the kinetics of albumin-triggered release, while Fig. 5e illustrates how this process correlates with intracellular ROS generation, a marker of therapeutic activity. *In vivo* tumor suppression data (Fig. 5f) validated its promise as a low-toxicity, sustained delivery strategy. Mi and co-workers expanded the design space by introducing fluorine-rich COFs, achieving remarkably high drug loading (*e.g.*, 69% for 5-FU) and efficient release under physiological conditions.[123] Similarly, Das *et al.* developed a robust 3D COF (TUS-84) with 2-fold interpenetrated scu net, showing strong stability and controlled ibuprofen release—highlighting how framework dimensionality and interpenetration can directly enhance therapeutic utility.[124] Morphological control was advanced by Chen *et al.*, who realized uniform hollow spherical COFs *via* a self-templating Ostwald ripening mechanism.[125] These spheres exhibited very high porosity and exceptional ibuprofen loading, along with excellent biocompatibility (Fig. 5g). This work showed how particle shape and internal architecture can be systematically engineered for optimal drug encapsulation and release kinetics. Dong *et al.* further introduced redox-sensitive porphyrin COFs containing disulfide linkages that degraded in glutathione-rich tumor microenvironments.[126] This enabled dual therapy—releasing 5-FU selectively in tumor cells while simultaneously enhancing photodynamic therapy through GSH depletion. Such logic-gated strategies represent an evolution toward multifunctional, synergistic nanotherapeutics. Beyond passive carriers, COFs are now being explored as active micromachines. Using light as an external trigger, two types of COF microswimmers were developed—spherical TAPB-PDA-COFs and porous TpAzo-COFs.[127] Their motion under visible light

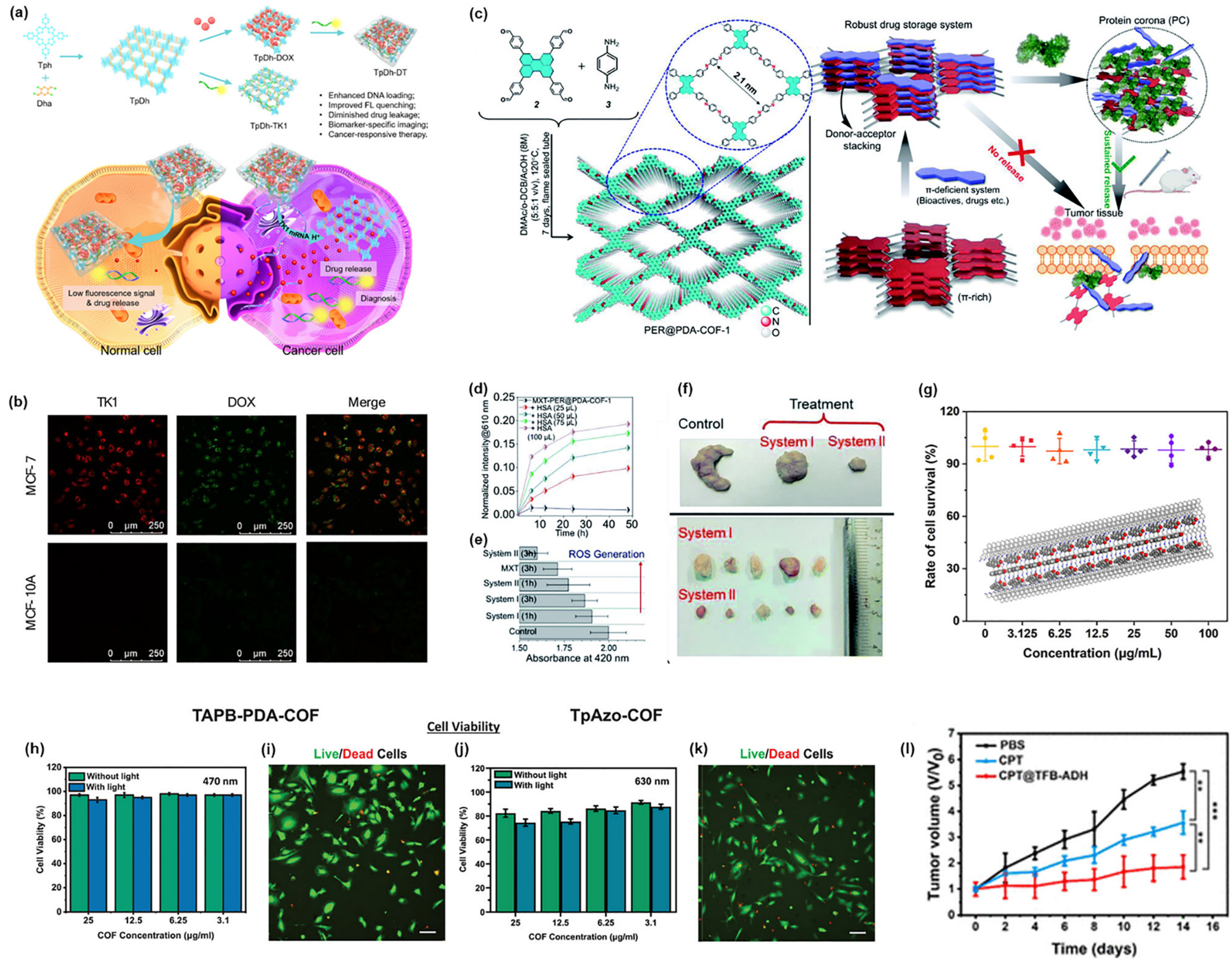

Fig. 5 (a) Preparation route and therapeutic applications of TpDh-DT. (b) Confocal visualization of TpDh-DT uptake in MCF-7 and MCF-10A cells. Adapted with permission from ref. 120. Copyright 2021 American Chemical Society. (c) Design of PER@PDA-COF-1 highlighting donor–acceptor based drug loading and albumin-triggered release mechanism. (d) Drug release profiles of MXT–PER@PDA-COF-1 and HSA–MXT–PER@PDA-COF-1 with varying albumin concentrations. (e) Intracellular ROS generation kinetics. (f) Tumor inhibition outcomes shown by excised tumor images. Adapted with permission from ref. 122. Copyright 2022 Creative Commons CC BY-NC 3.0. (g) Cytotoxicity of HAPTP-TPA COFs with drug confinement (inset: ibuprofen in COF channel). Adapted with permission from ref. 125. Copyright 2023 American Chemical Society. (h)–(k) Biocompatibility and photodynamic cytotoxicity of COF microswimmers. Adapted with permission from ref. 127. Copyright 2023 The Authors. Advanced Materials published by Wiley-VCH GmbH. (l) Tumor progression in mice under different therapeutic conditions. Adapted with permission from ref. 131. Copyright 2023 American Chemical Society.

facilitated drug transport in complex biological fluids. Biocompatibility studies with endothelial cells (Fig. 5h and i) confirmed the safety of spherical COFs, while TpAzo-COFs displayed somewhat lower tolerability (Fig. 5j and k). These findings point to COFs as programmable drug carriers capable of autonomous navigation. From a topological design perspective, Negishi and co-workers synthesized TUS-64, a 3D non-interpenetrated stp topology COF with record-large pore size (47 Å) and ultralow density, enabling efficient and controlled loading of multiple therapeutic molecules.[128] Follow-up work yielded interpenetrated pts topology COFs (TUS-440, TUS-441) that achieved sustained release of cytarabine and 5-FU, promising to reduce dosing frequency in chemotherapy.[129] Other groups have emphasized surface chemistry and morphology for responsive behavior. Yang *et al.* developed flower-shaped COFs (FSCOFs) encapsulated with hyaluronic acid, achieving dual pH and GSH responsiveness and efficient DOX delivery into cancer cells.[130] Weng *et al.* fabricated red-emissive COF nanospheres (COFNSs) that allowed real-time tracking of uptake, drug release, and apoptosis.[131] This was vividly demonstrated in tumor-bearing mice (Fig. 5l), where CPT-loaded COFNSs significantly reduced tumor burden. pH-responsive designs continue to provide robust therapeutic control. Kumar *et al.* validated that COF-LZU-1 achieves acid-triggered release with minimal leakage at neutral pH,[132] while Yang *et al.* introduced hydrazone-functionalized NCOFs where drug release was covalently gated and triggered under acidic tumor conditions,[133] further stabilized with phospholipid coatings for improved dispersibility and biocompatibility.

4.6 Applications of COFs in diverse preclinical models

While early studies of COFs as drug carriers focused predominantly on single-tumor xenograft models, recent work has begun to explore a broader spectrum of disease paradigms and animal species—illustrating the versatility of COFs beyond conventional oncology applications. Below we summarize representative studies across different disease types, species, routes of administration and therapeutic strategies.

4.6.1 COFs for metabolic disease: oral insulin delivery in diabetic models. A notable non-oncology application is the use of a triazine-based nanoscale COF, TTA-DFP-nCOF, for oral insulin delivery in diabetic rats. In this report, the authors demonstrated strong insulin-loading capacity ($\approx$65 wt%), stability of the COF in acidic gastric conditions, protection of insulin against degradation, and a glucose-responsive ''on-off'' insulin release mechanism *in vitro*. Upon oral administration in streptozotocin-induced type-1 diabetic rats, TTA-DFP-nCOF/insulin resulted in rapid normalization of blood glucose levels within 2 h and sustained glucose homeostasis for up to 10 h, comparable to non-diabetic controls, with no detectable systemic toxicity or organ pathology (liver and kidney histology remained normal) after treatment. These findings highlight that COFs can be viable carriers for hormone/peptide therapeutics *via* non-invasive administration routes, expanding their potential beyond cancer applications.[134] More recently, this concept has been independently reinforced through the development of a template-free self-assembled hollow microtubular COF (MT-COF-18 Å) designed specifically for insulin delivery.[135] In this work, hollow COF microtubules were obtained *via* controlled solvent-mediated self-assembly, yielding a well-defined macrostructure that combines ordered porosity with a hollow interior. This architecture enabled high insulin loading, pronounced gastroresistance, and glucose-responsive release behavior, addressing key challenges associated with oral peptide delivery. Detailed mechanistic studies revealed morphology evolution during insulin loading and release, confirming the structural adaptability of the COF host. Furthermore, surface functionalization with transferrin significantly enhanced insulin uptake and transcellular transport across Caco-2 cell monolayers, indicating improved intestinal permeability. *In vivo* experiments in diabetic rats demonstrated sustained glycemic control and therapeutically relevant blood insulin concentrations following oral administration, without observable systemic toxicity.

4.6.2 COFs in cancer therapy—beyond single tumor type, toward multimodal and metastatic models. • Although many COF-based studies use standard subcutaneous or orthotopic tumor models, engineered COF platforms are beginning to explore more challenging and clinically relevant tumor types. For instance, a recent report engineered a COF–SPION (superparamagnetic iron oxide nanoparticle) hybrid nanoplatform that delivered a chemotherapeutic agent in a targeted manner to tumor cells *via* a MUC1-specific aptamer, combining imaging (MRI) with therapy (theranostics) *in vivo*.[136]

• Another promising direction involves light-driven COF microswimmers—*e.g.*, imine-linked TABP-PDA-COF and azo-linked TpAzo-COF—which have been demonstrated to load insoluble drugs, navigate biological fluids, and release payloads under external stimulation (light), thereby offering a route toward enhanced tumor penetration, controlled release, and possibly deeper tissue distribution, potentially beneficial for poorly perfused or metastatic tumors.[127]

• The modularity of COF chemistry and surface functionalization (*e.g.*, targeting ligands, PEGylation, stimuli-sensitive linkages) support adaptation of COFs to diverse tumor microenvironments, including metastatic niches, hypoxic regions, or tumors with heterogeneous vascularization—offering opportunities for more systematic investigation across tumor types, metastatic models, and drug resistance contexts.

4.6.3 Emerging applications beyond cancer and diabetes—toward infection, inflammation, and theranostics. • While still in early stages, COFs are being investigated for theranostic applications: combining drug delivery with imaging or responsive release. For example, some COF-based carriers embed photosensitizers or photothermal agents to enable light-activated therapy, which may be extended to inflammation or localized infection models, where controlled activation can minimize systemic side effects.[137,138]

• The inherent modularity of COFs—in terms of pore geometry, linkage chemistry, surface functionalization—offers a promising platform for designing carriers tailored to unique disease contexts (*e.g.*, delivering anti-inflammatory drugs to inflamed tissues, antibiotics to infection sites, or immunomodulators to immune-privileged organs). Though systematic *in vivo* exploration is currently limited, this potential justifies the inclusion of non-oncology preclinical models in future COF research efforts.

4.6.4 Gaps and needs—toward long-term, multi-model, multi-species preclinical studies. Despite these promising developments, current COF studies remain heavily biased toward single tumor xenograft models or short-term metabolic disease models (*e.g.*, diabetic rats). Key gaps remain:

• Limited diversity of disease models—Few studies systematically compare COF performance across different tumor types (*e.g.*, lung, liver, pancreatic, metastatic), or in non-tumor diseases (*e.g.*, chronic inflammation, infection, autoimmune).

• Narrow species scope—Most *in vivo* work uses mice or rats; studies in larger mammals (*e.g.*, rabbits), or species with immune systems closer to humans, are largely absent.

• Lack of standardization in experimental design—Important parameters such as dosage, administration route, dosing frequency, and long-term efficacy/safety tracking are often not consistently reported or sufficiently explored.

• Insufficient long-term safety and biodistribution data—Few studies include long-term organ accumulation, immunogenicity, or repeated-dose toxicity evaluations, which are critical for clinical translation.

These gaps suggest a pressing need for future COF research to adopt a systematic, multi-model, multi-species preclinical

Table 2 Comparative performance metrics of COFs *versus* mainstream nanocarriers

Metric	Representative values across carriers
Drug loading efficiency	**COFs:** Typically 20–35 wt% (*e.g.*, TpPa-1: ~30 wt% 5-FU) **Liposomes:** Often <10 wt% (*e.g.*, DOX ~5–8 wt%) **MSNs:** ~15–25 wt% depending on pore size **Polymeric micelles:** Generally 5–15 wt%
Release controllability	**COFs:** Highly tunable (pH-, redox-, light-triggered), multistage gating *via* linkages or functional groups **Liposomes:** Mainly pH- or temperature-sensitive **MSNs:** Gatekeeper-dependent; moderate kinetics **Polymeric micelles:** Sensitive to pH/redox but often premature dissociation in serum
In vivo circulation half-life	**COFs:** Typically short for bare COFs ($t^{\frac{1}{2}} < 2$ h); PEGylation extends to 6–12 h **Liposomes:** Long-circulating formulations ($t_{\frac{1}{2}}$ 12–24 h) **MSNs:** Rapid clearance unless heavily modified **Polymeric micelles:** ~3–10 h
Biosafety & biocompatibility	**COFs:** Low hemolysis (<2% for COF-HQ), minimal hepatotoxicity in mouse models **Liposomes: Excellent safety; several FDA-approved** **MSNs:** Dose-dependent inflammation and oxidative stress **Polymeric micelles:** Some PEG-PLA and PEG-PCL formulations show >5% hemolysis
Scalability & production cost	**COFs:** Currently batch-to-batch variation; solvothermal methods costly at scale **Liposomes:** Established GMP manufacturing; economical **MSNs:** Large-scale synthesis feasible but costly surface modification **Polymeric micelles:** Scalable but purity control needed

strategy, including chronic dosing, biodistribution and toxicity studies, and disease-specific efficacy testing beyond canonical tumor models. In light of this, we strongly encourage the community to expand preclinical testing of COF-based carriers across a broader spectrum of disease models (metabolic disease, infection, inflammation, metastasis), animal species, and dosing regimens. Such comprehensive studies will be essential to validate the translational potential of COFs for diverse therapeutic applications.

4.7 Comparative analysis of COFs and mainstream nanocarriers

To help place COFs in the broader translational landscape, we provide a structured comparison against three mainstream nanocarrier classes (liposomes, MSNs, and polymeric nanoparticles) across five practical dimensions: drug-loading efficiency, release controllability, *in vivo* circulation/PK, biosafety, and manufacturability/cost. Table 2 provides a consolidated overview of these metrics. Wherever applicable, we include value ranges and representative case studies to illustrate comparative trends. Given the variability in experimental protocols across reports, ranges are used in place of single-point values, and direct side-by-side comparisons should be performed when precise benchmarking is needed.

5. Strategic vision for future research

The field of COFs as precision nanocarriers for targeted drug delivery is still in its formative stage, yet the convergence of reticular chemistry, nanomedicine, and molecular targeting is poised to drive transformative advances. While recent progress has been remarkable, several scientific and technological hurdles must be overcome to realize the clinical translation of COF-based drug delivery systems. The following key directions merit focused attention:

(1) **Scalable and reproducible synthesis without compromising structural precision:** Clinical translation requires COFs to be produced in gram-scale quantities with consistent particle size, morphology, crystallinity, and functional group distribution. Current synthetic routes often involve solvothermal conditions with long reaction times and low throughput, which are incompatible with pharmaceutical manufacturing requirements. Future efforts should prioritize continuous-flow or mechanochemical synthesis to achieve rapid, energy-efficient production while retaining atomic precision. Moreover, the ability to reproducibly incorporate targeting ligands, stimuli-responsive functionalities, and biocompatible coatings during large-scale synthesis will be essential for ensuring batch-to-batch consistency in therapeutic performance. Integration of green chemistry principles—such as aqueous-phase synthesis and recyclable catalysts—will further improve scalability and regulatory compliance.

(2) **Enhancing stability in physiological environments while enabling controlled degradation:** Although many COFs exhibit excellent thermal and chemical stability, their long-term structural integrity under physiological pH, ionic strength, and enzymatic conditions remains a critical concern. Future designs must balance structural robustness with the capacity for controlled, stimuli-triggered degradation into non-toxic byproducts after fulfilling their therapeutic function. Strategies may include incorporating cleavable linkages (*e.g.*, ester, imine, hydrazone) that respond to tumor-associated pH or enzymatic activity, while ensuring that the framework remains intact during circulation. A deeper understanding of how framework topology, linker hydrophobicity, and

interlayer interactions influence stability in biological fluids will guide the rational design of COFs tailored for *in vivo* drug delivery.

(3) Comprehensive PK and biodistribution profiling: To accelerate the clinical translation of COF-based drug delivery systems, it is essential to establish a rigorous and standardized PK and biodistribution evaluation framework tailored to the unique structural and degradation characteristics of COFs. Unlike conventional organic nanoparticles, COFs possess permanent porosity, variable crystallinity, and diverse linker–node chemistries, which may generate distinct absorption, distribution, metabolism, and excretion (ADME) behaviors. Currently, only a few *in vivo* studies have reported PK profiles of COFs, leaving critical knowledge gaps regarding their long-term fate and safety.

A systematic evaluation system should integrate:

(i) Size-, shape-, and surface-property–dependent PK assessment, examining how hydrodynamic diameter, topology, zeta potential, and functional group density influence interactions with plasma proteins, endothelial barriers, and immune components. For instance, ultrasmall COFs (<10 nm) may undergo rapid renal filtration, whereas larger particles (≥ 50–150 nm) may exhibit extended circulation but require strategies to minimize sequestration by the mononuclear phagocyte system (MPS/RES).

(ii) Biodegradation and metabolic fate analysis, including tracking of linker cleavage, metal-node dissolution (in metalated COFs), and formation of soluble or insoluble metabolites. LC–MS, ICP–MS, untargeted metabolomics, and excretion profiling (urine, feces, bile) should be employed to differentiate intact COFs from degraded products.

(iii) Spatiotemporal biodistribution mapping, integrating multimodal imaging tools such as PET/SPECT (radiolabelled COFs), MRI (paramagnetic nodes), photoacoustic imaging, and fluorescence lifetime imaging to enable quantitative, real-time tracking at organ, tissue, and cellular levels.

(iv) Immune and hematological compatibility profiling, including complement activation (CARPA), cytokine response, immunogenicity, and macrophage uptake kinetics, which are critical for repeated-dosing regimens.

(v) Physiologically based pharmacokinetic (PBPK) modeling, to predict human-relevant PK parameters by incorporating COF-specific attributes—pore architecture, degradation rate, payload release kinetics, and protein corona evolution.

(4) Rational engineering for active targeting and biomarker-specific delivery: The reticular chemistry toolbox uniquely enables the spatially precise incorporation of targeting ligands—such as peptides, aptamers, antibodies, or small molecules—into COF pores or backbones. Future research should exploit this feature to engineer COFs that recognize disease-specific biomarkers with high selectivity, enabling accumulation at pathological sites while sparing healthy tissues. In cancer therapy, for instance, targeting overexpressed receptors (*e.g.*, folate receptor α, HER2, or integrins) could enhance tumor uptake and therapeutic efficacy. A promising avenue lies in multiplex targeting, wherein COFs are functionalized with multiple ligands to address tumor heterogeneity and improve binding efficiency across diverse cell populations.

(5) Development of multi-drug and multi-modal delivery systems: The large, tunable pore volumes and modular chemistry of COFs open unique opportunities for co-delivery of multiple therapeutic classes, and for the fusion of advanced therapeutic modalities beyond classical drugs and imaging agents. Future platforms should therefore not only (i) integrate small-molecule chemotherapeutics with macromolecular biologics (siRNA, mRNA, or CRISPR–Cas9), but also (ii) embed immune modulation, and (iii) interface with microbial therapies. By doing so, COFs can evolve into true multi-modal theranostic systems that combine therapy, diagnosis, real-time monitoring, and synergistic mechanistic combinations.

COF-mediated gene-editing delivery. COFs functionalised with amine, guanidinium or other reactive moieties (for example, an APTES-modification of COF-1) can serve as robust carriers for CRISPR–Cas9 plasmids or ribonucleoproteins (RNPs). The rigid pore structure protects the genetic cargo, while pH- or redox-responsive linkers allow controlled release in tumour micro-environments. Although direct COF-CRISPR studies are still nascent, broader nanoparticle work suggests editing efficiencies approaching ~40–50% indel/knockout in model systems when payload delivery is optimised.[139,140] However, a major challenge remains the creation of sufficiently large pores in COFs to accommodate high-molecular-weight biomolecules such as Cas9 or other therapeutic proteins, which necessitates careful topology and linker design to expand pore size without compromising structural stability. In future COF designs, key parameters such as pore size, surface charge, linker density, nuclear-localisation peptide integration and off-target profiling must be systematically explored. Imaging reporters (*e.g.*, fluorescent Cas9 tracers) could be integrated into the COF core to allow live-cell monitoring of editing events.

Synergistic COF–immunotherapy platforms. Beyond imaging/phototherapy, COFs can be engineered for immune-modulatory work: *e.g.*, surface-anchored immune checkpoint antibodies (anti-PD-L1 or anti-PD-1) combined with chemotherapeutics loaded in the pore cavities. In one reported nanoparticle system (not yet COF-based), decitabine and paclitaxel were co-delivered in a PD-L1-targeted formulation that enhanced tumor accumulation, reversed paclitaxel resistance, and remodelled the immune microenvironment to boost anti-tumor T-cell activity.[141] By adapting this into COF chemistry, one could exploit high loading capacity + precise spatial arrangement of functional groups to produce immunogenic cell death, reverse tumour immune-suppression and enable immunological memory. Future work should measure effector markers (IFN-γ, granzyme B), memory T-cell subpopulations, and durability of response in immunocompetent animal models.

COF integration with bacteriotherapy (microbiome/modulation). COFs may also encapsulate live microorganisms or engineered probiotic strains for gut-targeted delivery—expanding beyond classic drug carriers into microbiome-therapeutics. For example, a recent study encapsulated microbes in a COF-based artificial probiotic shell for inflammatory-bowel-disease treatment, demonstrating enhanced survival and immunomodulation.[142] Future COF systems could expressly tune shell porosity, pH-responsiveness (intestinal release), and payload (probiotic + metabolite + immunomodulator), and assess survival rates, colonisation kinetics, microbiota shifts, and inflammation biomarkers *in vivo*.

(6) **Advanced stimuli-responsive and logic-gated release mechanisms:** Stimuli-responsive COFs—capable of releasing cargo in response to pH, temperature, enzymatic activity, redox potential, or light—hold immense promise for on-demand drug delivery. Future work should move toward multi-stimuli and logic-gated release systems, where drug release occurs only when multiple disease-specific conditions are met. Such Boolean "AND" or "OR" logic release mechanisms could significantly enhance specificity, reducing premature drug leakage and minimizing systemic toxicity. Integration of photo-responsive linkers, disulfide bonds, or enzyme-cleavable peptides into the COF backbone could further refine spatiotemporal control over therapeutic delivery.

(7) **Hybrid and composite COF nanocarriers for synergistic functionality:** Combining COFs with other nanomaterials—such as gold nanoparticles, liposomes, polymeric micelles, or magnetic nanoparticles—could yield hybrid carriers that harness the best features of each component. For instance, COF–liposome hybrids might improve circulation time and immune evasion, while COF–magnetic composites could enable magnetically guided drug targeting. Such hybrid systems should be designed to maintain the crystalline precision of the COF framework while integrating functionalities that improve bioavailability, targeting, and endosomal escape.

(8) **Integrating computational modelling to predict drug binding, transport, and COF design:** To truly harness the potential of COFs as precision nanocarriers, future research should embed multiscale computational modelling into the design–test cycle. We envision this along three interlinked dimensions:

Molecular-level simulations of drug–COF interactions

• Use molecular dynamics (MD) simulations (and where needed, enhanced sampling techniques) to model the binding conformations, energetics, and release pathways of drug molecules within COF pores. For example, in a porphyrin-based COF (COF-366), MD combined with density functional theory (DFT) has been used to compute adsorption free energies of DOX and irinotecan (IRI) (~ -20 kcal mol^{-1}), primarily driven by π–π stacking interactions.[143]

• Complement this with quantum chemical calculations (*e.g.*, DFT, NBO, QTAIM) to characterize the nature and strength of specific non-covalent interactions (π–π, hydrogen bonding, electrostatics) and to estimate barriers for desorption or diffusion.

• Validate with ML models: for instance, Yadav *et al.* recently used MD/GCMC data + deep neural networks to predict 5-FU adsorption in a database of >1200 COFs, identifying key structure–property relationships such as accessible surface area, void fraction and chemical descriptors.[144]

• Through combined theory and ML, one can rationalize why certain COFs exhibit negligible leakage: *e.g.*, a strongly negative binding energy (~ -20 kcal mol^{-1}) or a tight radial distribution function between drug and pore lining can explain very slow release.

Multiscale simulations of in vivo transport and pharmacokinetic behavior

• Employ computational fluid dynamics (CFD) or lattice Boltzmann–immersed boundary (LB–IB) methods to simulate nanoparticle transport in the bloodstream, accounting for realistic flow conditions, shear stresses, and endothelial interactions. While such modelling has been done for other nanoparticle systems, *e.g.*, CFD models simulating the effect of interstitial fluid pressure and blood–tumor barrier transport of nanoparticles,[145] these methods could be extended to COFs.

• Build mesoscopic/continuum models (*e.g.*, PBPK) which incorporate inputs from CFD (circulation half-life, margination, aggregation) and molecular simulations (binding, degradation, payload release) to predict systemic – and organ-level – PK of COF formulations.

• Validate model predictions: for example, if the model suggests that PEGylated COFs will have a circulation half-life of ∼6 h under physiological shear, one would compare that with *in vivo* PK experiments in appropriate animal models (*e.g.*, mice) to verify circulation time, tissue accumulation, and clearance routes.

Machine learning–assisted rational design of COFs

• Build predictive ML models (*e.g.*, random forest, DNN) that correlate COF descriptors (linkage chemistry, pore size/limiting diameter, topology, functional groups) with experimentally measured drug loading, release kinetics, and stability. For instance, the recent study used a database of 1242 COFs to train ML to predict 5-FU loading capacity, achieving good predictive accuracy.[144]

• Use feature-importance methods (*e.g.*, SHAP) to identify which structural descriptors (*e.g.*, linker types, carbon/nitrogen content, surface area, void fraction) most strongly influence drug loading and release behavior. This helps uncover design rules, such as which linkage chemistries (*e.g.*, imine *vs.* triazine) or pore dimensions maximize retention or enable controlled release.

• Use the model to screen novel COFs *in silico* before synthesis. By applying the trained model to virtual libraries of hypothetical COF structures, researchers can rapidly prioritize candidates with optimal predicted loading capacities, release kinetics, and physicochemical stability, thereby narrowing the design space and significantly reducing time- and resource-intensive experimental synthesis and testing cycles.

(9) **Evaluating long-term biosafety, chronic toxicity, and immunogenicity:** A comprehensive understanding of the biosafety of COFs is indispensable for their clinical translation. While most studies have focused on short-term cytotoxicity using 2D cell cultures (*e.g.*, MTT or live/dead assays), long-term toxicity and immunogenicity arising from *in vivo* accumulation—particularly in the liver, spleen, and kidneys—remain insufficiently characterized. Future investigations should adopt chronic exposure models and longitudinal biodistribution

analyses to assess retention, metabolism, and clearance over extended timeframes (weeks to months). Accepted guidelines such as the OECD Repeated Dose 28-Day Oral Toxicity Study in Rodents (Test Guideline 407)[146] offer useful frameworks for nanoparticle systems. Appropriate animal models—such as BALB/c or C57BL/6 mice for immune profiling, Sprague–Dawley rats for systemic toxicity, and zebrafish or organ-on-chip systems for early-stage screening—should be employed.

Key detection indicators should include hematological and biochemical markers (ALT, AST, BUN, creatinine), oxidative stress parameters (ROS, MDA, GSH levels), and proinflammatory cytokines (IL-6, TNF-α, IL-1β) to monitor systemic responses. Histopathological examination of major organs (liver, spleen, lung, kidney, and heart) is essential to detect tissue accumulation or fibrosis. Advanced imaging modalities—such as PET, MRI, ICP-MS mapping, and fluorescence tomography—should be applied to visualize the biodistribution and clearance pathways of COFs in real time.

Moreover, immunogenicity evaluation should include complement activation (C3a, C5a), antibody production (IgM, IgG titers), and immune cell profiling *via* flow cytometry to quantify macrophage or T-cell activation. These multi-level assays will provide mechanistic insight into how particle size, surface chemistry, and degradation products influence immune recognition. Finally, the establishment of standardized protocols for long-term biosafety evaluation—including dosage frequency, observation period, and recovery studies—will be crucial for regulatory acceptance and comparison across different COF platforms.

Despite the promising therapeutic potential of COF-based nanocarriers, several fundamental barriers continue to impede their clinical translation. First, the physiological stability and degradation behavior of COFs *in vivo* remain insufficiently understood; frameworks must retain structural integrity during circulation yet degrade into safe, excretable fragments after drug release, but only a few studies provide quantitative degradation kinetics or identify metabolic byproducts. Second, pharmacokinetics, biodistribution, and clearance pathways are still unclear compared with established nanocarriers such as liposomes or polymeric nanoparticles, and regulators require predictable organ distribution and elimination profiles before clinical approval. Third, scalability and reproducibility challenges persist: most COFs are synthesized under conditions difficult to translate into GMP-compliant, large-scale manufacturing, resulting in batch-to-batch variability in particle size, crystallinity, and surface functionality. Finally, standardized protocols, toxicity databases, and regulatory frameworks specific to COFs are still lacking, which complicates risk assessment and delays the establishment of clinical development pipelines. Addressing these scientific, technological, and regulatory gaps is essential for advancing COFs from preclinical research toward real-world clinical application.

(10) Industrialization, quality control, and regulatory outlook for COF-based drug delivery:

Key industrial bottlenecks. The successful translation of COF nanocarriers will depend on overcoming manufacturing and regulatory hurdles. First, controlling COF particle-size uniformity during large-scale synthesis is crucial: whereas laboratory-scale batches may achieve variation $<5\%$, industrial upscaling frequently results in size variation $>15\%$. Robust quality-control standards must therefore be established to ensure batch-to-batch reproducibility and consistent therapeutic performance. Essential parameters that should be standardized include (i) particle size and morphology analyzed *via* dynamic light scattering (DLS) and transmission electron microscopy (TEM), (ii) surface area and pore structure validated using Brunauer–Emmett–Teller (BET) measurements and small-angle X-ray scattering (SAXS), (iii) drug loading and encapsulation efficiency, (iv) framework crystallinity and purity using powder X-ray diffraction (PXRD) and Fourier transform infrared (FTIR) spectroscopy, and (v) surface chemistry and functional-group retention verified by X-ray photoelectron spectroscopy (XPS) and NMR spectroscopy. Implementing these as Critical Quality Attributes (CQAs) under Good Manufacturing Practice (GMP) protocols will enable comparability between batches and regulatory acceptance. Standard operating procedures (SOPs) for COF synthesis, purification, and post-synthetic modification should be documented with traceable batch records. Real-time process analytical technologies (PATs)—such as in-line Raman or IR spectroscopy—could be employed to monitor reaction kinetics and defect formation during synthesis. Furthermore, statistical process control (SPC) and acceptance criteria ($\pm 10\%$) for key physicochemical parameters must be established, similar to FDA and ICH guidelines for nanomaterial-based pharmaceuticals. Second, standardizing accelerated stability testing for drug–COF complexes is required: protocols involving defined temperature/humidity (*e.g.*, 40 °C/75% RH over 6 months) should be adopted to emulate long-term storage and physiological conditions. Third, establishing production-cost benchmarks is essential: for example, gram-scale solvothermal COF synthesis may cost $\sim\$50\ g^{-1}$, whereas mechanochemical routes could reduce this to $\sim\$10\ g^{-1}$. Economic modelling of cost–performance parameters will inform decisions about manufacturability.

Regulatory strategy recommendations. Drawing on the U.S. Food and Drug Administration (FDA)'s guidance[147] for nanomaterial-containing drug products, developers should identify critical quality attributes (CQAs) for COF nanocarriers—such as particle-size distribution, impurity content and degradation-product identification—and consult regulators early in the development process. A "COF Material Safety Database" to aggregate toxicity, immunogenicity and long-term-degradation data across different link-type COFs is proposed to inform regulatory pathways and enable standardized approval criteria. Additionally, transparent manufacturing traceability, Good Manufacturing Practice (GMP) compliance and post-market surveillance plans are imperative.

A comprehensive summary of the central strategies and priority areas for COF-based drug nanocarriers is provided in Fig. 6. In summary, the next decade will likely witness a transition from laboratory-scale demonstrations of COF drug carriers toward clinically viable, precision-engineered

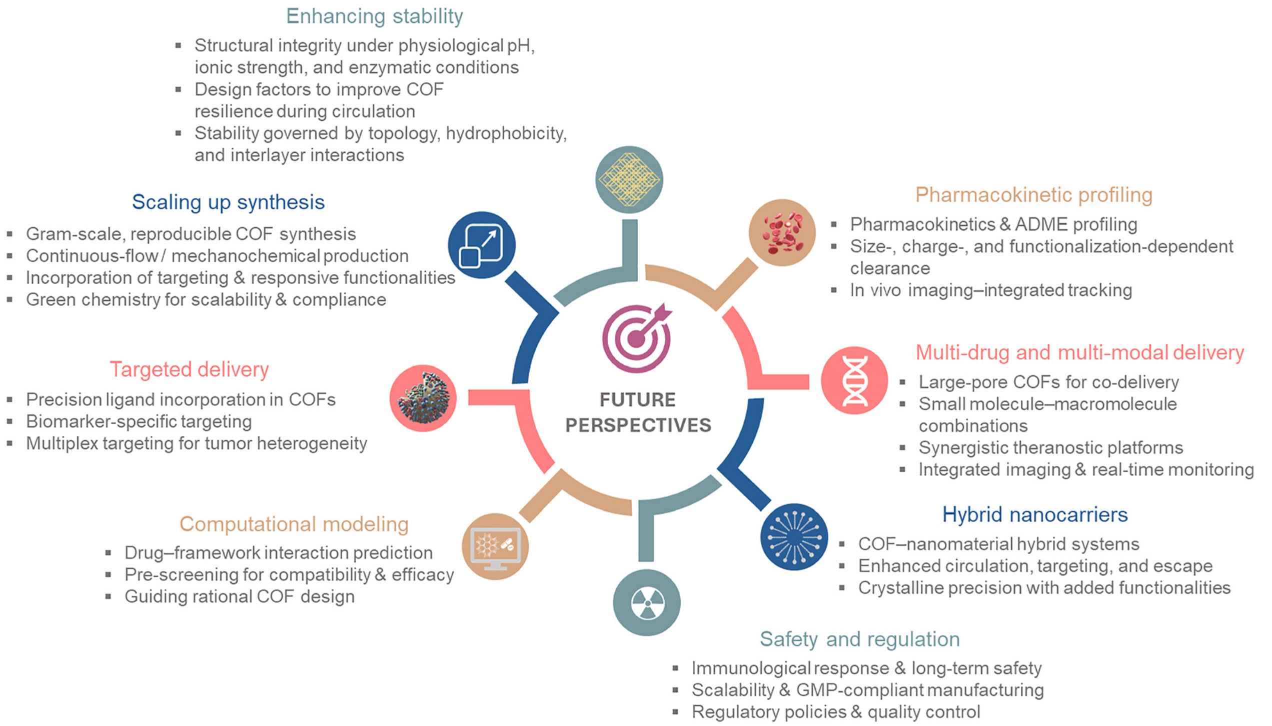

Fig. 6 Envisioned strategies and priorities in COF-based drug nanocarriers.

nanomedicines. Achieving this will require integrated advances in framework design, large-scale synthesis, biological evaluation, and regulatory compliance. By uniting the structural precision of reticular chemistry with the demands of modern nanomedicine, COFs have the potential to redefine the landscape of targeted and personalized drug delivery.

6. Conclusions

COFs have emerged as a highly versatile and structurally tunable platform for drug delivery, offering unparalleled control over porosity, functionality, and stability. Their modular and crystalline architectures allow precise incorporation of therapeutic cargos, enabling controlled release profiles and targeted delivery strategies that can be tailored to specific disease contexts, including oncology. The intrinsic chemical stability and biocompatibility of COFs, combined with their ability to integrate with other nanomaterials or stimuli-responsive components, position them as next-generation vectors for precision medicine. Recent advances demonstrate that judicious design of COF topology, functional groups, and host–guest interactions can significantly enhance drug loading, release kinetics, and cellular uptake, highlighting structure–function correlations that are essential for clinical translation. Looking forward, the integration of COFs with emerging modalities—such as immunotherapy, gene therapy, and multimodal imaging—holds substantial promise for developing multifunctional therapeutic platforms. Continued research at the interface of materials chemistry, pharmacology, and nanomedicine is poised to unlock the full potential of COFs, establishing them as a cornerstone in the rational design of next-generation drug delivery systems.

Conflicts of interest

There are no conflicts to declare.

Data availability

No primary research results, software or code have been included and no new data were generated or analysed as part of this review.

Acknowledgements

This study was supported by the Scientific Research on Innovative Areas "Aquatic Functional Materials" (grant no. 22H04562), JSPS KAKENHI (grant no. 23H00289 and 23KK0098), the Yazaki Memorial Foundation for Science and Technology, and the FUSO Innovative Technology Fund.

References

1 T. C. Ezike, U. S. Okpala, U. L. Onoja, C. P. Nwike, E. C. Ezeako, O. J. Okpara, C. C. Okoroafor, S. C. Eze, O. L. Kalu, E. C. Odoh, U. G. Nwadike, J. O. Ogbodo, B. U. Umeh, E. C. Ossai and B. C. Nwanguma, *Heliyon*, 2023, **9**, e17488.
2 N. Rahoui, B. Jiang, N. Taloub and Y. D. Huang, *J. Controlled Release*, 2017, **255**, 176–201.

3 A. M. Vargason, A. C. Anselmo and S. Mitragotri, *Nat. Biomed. Eng.*, 2021, **5**, 951–967.
4 L. L.-W. Wang, Y. Gao, Z. Feng, D. J. Mooney and S. Mitragotri, *Nat. Rev. Bioeng.*, 2024, **2**, 944–959.
5 J. Gao, J. M. Karp, R. Langer and N. Joshi, *Chem. Mater.*, 2023, **35**, 359–363.
6 M. W. Tibbitt, J. E. Dahlman and R. Langer, *J. Am. Chem. Soc.*, 2016, **138**, 704–717.
7 M. A. Beach, U. Nayanathara, Y. Gao, C. Zhang, Y. Xiong, Y. Wang and G. K. Such, *Chem. Rev.*, 2024, **124**, 5505–5616.
8 N. Kamaly, B. Yameen, J. Wu and O. C. Farokhzad, *Chem. Rev.*, 2016, **116**, 2602–2663.
9 K. Ulbrich, K. Holá, V. Šubr, A. Bakandritsos, J. Tuček and R. Zbořil, *Chem. Rev.*, 2016, **116**, 5338–5431.
10 J. Kumar Patra, G. Das, L. F. Fraceto, E. V. R. Campos, M. D. P. Rodriguez-Torres, L. S. Acosta-Torres, L. A. Diaz-Torres, R. Grillo, M. K. Swamy, S. Sharma, S. Habtemariam and H.-S. Shin, *J. Nanobiotechnol.*, 2018, **16**, 71.
11 M. C. Scicluna and L. Vella-Zarb, *ACS Appl. Nano Mater.*, 2020, **3**, 3097–3115.
12 B. S. Pattni, V. V. Chupin and V. P. Torchilin, *Chem. Rev.*, 2015, **115**, 10938–10966.
13 Z. Ahmad, A. Shah, M. Siddiqa and H.-B. Kraatz, *RSC Adv.*, 2014, **4**, 17028–17038.
14 P. Zrazhevskiy, M. Sena and X. Gao, *Chem. Soc. Rev.*, 2010, **39**, 4326–4354.
15 M. Vallet-Regí, F. Schüth, D. Lozano, M. Colilla and M. Manzano, *Chem. Soc. Rev.*, 2022, **51**, 5365–5451.
16 R. Zhang, Z. Yan, M. Gao, B. Zheng, B. Yue and M. Qiu, *J. Mater. Chem. B*, 2024, **12**, 12437–12469.
17 J. Grimm and D. A. Scheinberg, *Semin. Radiat. Oncol.*, 2011, **21**, 80–87.
18 G. Yang, S. Z. F. Phua, A. K. Bindra and Y. Zhao, *Adv. Mater.*, 2019, **31**, 1805730.
19 R. Mohammapdour and H. Ghandehari, *Adv. Drug Delivery Rev.*, 2022, **180**, 114022.
20 S. Xiang, J. Liu, G. Han, W. Zhang, Y. Long, Y. Deng, B. Wang and Q. Weng, *Chem. Eng. J.*, 2023, **470**, 144177.
21 Y. Herdiana, N. Wathoni, S. Shamsuddin and M. Muchtaridi, *OpenNano*, 2022, **7**, 100048.
22 L. M. Russell, M. Hultz and P. C. Searson, *J. Controlled Release*, 2018, **269**, 171–176.
23 D. Chang, Y. Ma, X. Xu, J. Xie and S. Ju, *Front. Bioeng. Biotechnol.*, 2021, **9**, 707319.
24 J. V. Natarajan, C. Nugraha, X. W. Ng and S. Venkatraman, *J. Controlled Release*, 2014, **193**, 122–138.
25 O. M. Yaghi, M. J. Kalmutzki and C. S. Diercks, *Introduction to Reticular Chemistry: Metal-Organic Frameworks and Covalent Organic Frameworks*, Wiley-VCH, Weinheim, Germany, 2019, ch. 7–11, pp. 177–283.
26 T. Irie, S. Das, Q. Fang and Y. Negishi, *J. Am. Chem. Soc.*, 2025, **147**, 1367–1380.
27 K. T. Tan, S. Ghosh, Z. Wang, F. Wen, D. Rodríguez-San-Miguel, J. Feng, N. Huang, W. Wang, F. Zamora, X. Feng, A. Thomas and D. Jiang, *Nat. Rev. Methods Primers*, 2023, **3**, 1.
28 S.-Y. Ding and W. Wang, *Chem. Soc. Rev.*, 2013, **42**, 548–568.
29 F. Haase and B. V. Lotsch, *Chem. Soc. Rev.*, 2020, **49**, 8469–8500.
30 D. Blätte, F. Ortmann and T. Bein, *J. Am. Chem. Soc.*, 2024, **146**, 32161–32205.
31 S. Kandambeth, K. Dey and R. Banerjee, *J. Am. Chem. Soc.*, 2019, **141**, 1807–1822.
32 Y. Song, Q. Sun, B. Aguila and S. Ma, *Adv. Sci.*, 2019, **6**, 1801410.
33 X. Zhao, P. Pachfule and A. Thomas, *Chem. Soc. Rev.*, 2021, **50**, 6871–6913.
34 X. Han, C. Yuan, B. Hou, L. Liu, H. Li, Y. Liu and Y. Cui, *Chem. Soc. Rev.*, 2020, **49**, 6248–6272.
35 Y. Li, W. Chen, G. Xing, D. Jiang and L. Chen, *Chem. Soc. Rev.*, 2020, **49**, 2852–2868.
36 J. Á. Martín-Illán, D. Rodríguez-San-Miguel and F. Zamora, *Coord. Chem. Rev.*, 2023, **495**, 215342.
37 X. Li, P. Yadav and K. P. Loh, *Chem. Soc. Rev.*, 2020, **49**, 4835–4866.
38 A. P. Côté, A. I. Benin, N. W. Ockwig, M. O'Keeffe, A. J. Matzger and O. M. Yaghi, *Science*, 2005, **310**, 1166–1170.
39 I. E. Khalil, P. Das and A. Thomas, *Acc. Chem. Res.*, 2024, **57**, 3138–3150.
40 X. Guan, F. Chen, Q. Fang and S. Qiu, *Chem. Soc. Rev.*, 2020, **49**, 1357–1384.
41 X. Yang, Q. Xu, W. Wei and G. Zeng, *Angew. Chem., Int. Ed.*, 2025, **64**, e202504355.
42 F. Mehvari, V. Ramezanzade, P. Asadi, N. Singh, J. Kim, M. Dinari and J. S. Kim, *Aggregate*, 2024, **5**, e480.
43 Y. Shi, J. Yang, F. Gao and Q. Zhang, *ACS Nano*, 2023, **17**, 1879–1905.
44 H. Kaur, S. S. Siwal, R. V. Saini and V. K. Thakur, *ACS Omega*, 2024, **9**, 6235–6252.
45 P. Ghosh and P. Banerjee, *Chem. Commun.*, 2023, **59**, 12527–12547.
46 M.-J. Kang, Y.-W. Cho and T.-H. Kim, *Coord. Chem. Rev.*, 2025, **527**, 216400.
47 S. Mitra, H. S. Sasmal, T. Kundu, S. Kandambeth, K. Illath, D. Díaz Díaz and R. Banerjee, *J. Am. Chem. Soc.*, 2017, **139**, 4513–4520.
48 F. Benyettou, M. Khair, T. Prakasam, S. Varghese, Z. Matouk, M. Alkaabi, P. Pena-Sánchez, M. Boitet, R. AbdulHalim, S. K. Sharma, R. Ghemrawi, S. Thomas, J. Whelan, R. Pasricha, R. Jagannathan, F. Gándara and A. Trabolsi, *ACS Appl. Mater. Interfaces*, 2024, **16**, 56676–56695.
49 C. Wang, H. Liu, S. Liu, Z. Wang and J. Zhang, *Front. Chem.*, 2020, **8**, 488.
50 K. Sasaki, T. Irie, M. Nozaki, T. Kawawaki, S. Das and Y. Negishi, *Nanoscale Horiz.*, 2025, **10**, 3309–3318.
51 W.-R. Zhuang, Y. Wang, P.-F. Cui, L. Xing, J. Lee, D. Kim, H. L. Jiang and Y.-K. Oh, *J. Controlled Release*, 2019, **294**, 311–326.
52 M. D. DeFuria, M. Zeller and D. T. Genna, *Cryst. Growth Des.*, 2016, **16**, 3530–3534.

53 S. Akhzari, H. Raissi and A. Ghahari, *npj Clean Water*, 2024, **7**, 31.
54 J. Saksena, A. E. Hamilton, R. J. Gilbert and J. M. Zuidema, *Front. Cell. Neurosci.*, 2023, **17**, 1266019.
55 Y. Li, M. Kröger and W. K. Liu, *Nanoscale*, 2015, **7**, 16631–16646.
56 W. Zhang, R. Taheri-Ledari, F. Ganjali, S. S. Mirmohammadi, F. S. Qazi, M. Saeidirad, A. KashtiAray, S. Zarei-Shokat, Y. Tian and A. Maleki, *RSC Adv.*, 2023, **13**, 80–114.
57 N. R. Khalili, A. B. Dehkordi, A. Amiri, G. M. Ziarani, A. Badiei and P. Cool, *ACS Appl. Mater. Interfaces*, 2024, **16**, 28245–28262.
58 S. M. M. Moghadam, M. Ramezani, M. Alibolandi, K. Abnous and S. M. Taghdisi, *J. Drug Targeting*, 2025, 1–10, DOI: 10.1080/1061186X.2025.2527865.
59 H. M. El-Kaderi, J. R. Hunt, J. L. Mendoza-Cortés, A. P. Côté, R. E. Taylor, M. O'Keeffe and O. M. Yaghi, *Science*, 2007, **316**, 268–272.
60 F. J. Uribe-Romo, J. R. Hunt, H. Furukawa, C. Klöck, M. O'Keeffe and O. M. Yaghi, *J. Am. Chem. Soc.*, 2009, **131**, 4570–4571.
61 S. Kandambeth, A. Mallick, B. Lukose, M. V. Mane, T. Heine and R. Banerjee, *J. Am. Chem. Soc.*, 2012, **134**, 19524–19527.
62 F. J. Uribe-Romo, C. J. Doonan, H. Furukawa, K. Oisaki and O. M. Yaghi, *J. Am. Chem. Soc.*, 2011, **133**, 11478–11481.
63 S. J. Sonawane, R. S. Kalhapure and T. Govender, *Eur. J. Pharm. Sci.*, 2017, **99**, 45–65.
64 P. Kuhn, M. Antonietti and A. Thomas, *Angew. Chem., Int. Ed.*, 2008, **47**, 3450–3453.
65 Q. Fang, Z. Zhuang, S. Gu, R. B. Kaspar, J. Zheng, J. Wang, S. Qiu and Y. Yan, *Nat. Commun.*, 2014, **5**, 4503.
66 J. Guo, Y. Xu, S. Jin, L. Chen, T. Kaji, Y. Honsho, M. A. Addicoat, J. Kim, A. Saeki, H. Ihee, S. Seki, S. Irle, M. Hiramoto, J. Gao and D. Jiang, *Nat. Commun.*, 2013, **4**, 2736.
67 C. Zhao, C. S. Diercks, C. Zhu, N. Hanikel, X. Pei and O. M. Yaghi, *J. Am. Chem. Soc.*, 2018, **140**, 16438–16441.
68 P. J. Waller, S. J. Lyle, T. M. Osborn Popp, C. S. Diercks, J. A. Reimer and O. M. Yaghi, *J. Am. Chem. Soc.*, 2016, **138**, 15519–15522.
69 R.-Z. Li, S.-C. Yu, W. Jiang, J. Zhou, Z.-C. Wang, X.-R. Ren, W. Feng, Y. Zhou, D. Wang and L.-J. Wan, *J. Am. Chem. Soc.*, 2025, **147**, 31016–31024.
70 H. Lyu, C. S. Diercks, C. Zhu and O. M. Yaghi, *J. Am. Chem. Soc.*, 2019, **141**, 6848–6852.
71 B. Zhang, M. Wei, H. Mao, X. Pei, S. A. Alshmimri, J. A. Reimer and O. M. Yaghi, *J. Am. Chem. Soc.*, 2018, **140**, 12715–12719.
72 X. Guan, H. Li, Y. Ma, M. Xue, Q. Fang, Y. Yan, V. Valtchev and S. Qiu, *Nat. Chem.*, 2019, **11**, 587–594.
73 S. Zhang, X. Zhao, B. Li, C. Bai, Y. Li, L. Wang, R. Wen, M. Zhang, L. Ma and S. Li, *J. Hazard. Mater.*, 2016, **314**, 95–104.
74 D. Kurandina, B. Huang, W. Xu, N. Hanikel, A. Darù, G. D. Stroscio, K. Wang, L. Gagliardi, F. D. Toste and O. M. Yaghi, *Angew. Chem., Int. Ed.*, 2023, **62**, e202307674.
75 X. Han, Z. Zhou, K. Wang, Z. Zheng, S. E. Neumann, H. Zhang, T. Ma and O. M. Yaghi, *J. Am. Chem. Soc.*, 2024, **146**, 89–94.
76 L. Zhong, J. Liu, Y. Xiao, Z. Song, L. Chen, G. Li and Y. Wu, *Asian J. Pharm. Sci.*, 2025, **20**, 101066.
77 Z. Alsudairy, N. Brown, C. Yang, S. Cai, F. Akram, A. Ambus, C. Ingram and X. Li, *Precis. Chem.*, 2023, **1**, 233–240.
78 N. L. Campbell, R. Clowes, L. K. Ritchie and A. I. Cooper, *Chem. Mater.*, 2009, **21**, 204–206.
79 W. Zhao, X. Wang, M. Bahri, Q. Zhu, B. Li, K. Wu, Z. Wang, H. Li, X. Shi, D. Shi, C. Ji, N. D. Browning, J. Sun, J. Wang and D. Zhao, *J. Am. Chem. Soc.*, 2025, **147**, 16319–16330.
80 B. P. Biswal, S. Chandra, S. Kandambeth, B. Lukose, T. Heine and R. Banerjee, *J. Am. Chem. Soc.*, 2013, **135**, 5328–5331.
81 G. Das, D. B. Shinde, S. Kandambeth, B. P. Biswal and R. Banerjee, *Chem. Commun.*, 2014, **50**, 12615–12618.
82 S. Karak, S. Kandambeth, B. P. Biswal, H. S. Sasmal, S. Kumar, P. Pachfule and R. Banerjee, *J. Am. Chem. Soc.*, 2017, **139**, 1856–1862.
83 N. Brown, Z. Alsudairy, R. Behera, F. Akram, K. Chen, K. Smith-Petty, B. Motley, S. Williams, W. Huang, C. Ingram and X. Li, *Green Chem.*, 2023, **25**, 6287–6296.
84 S. T. Emmerling, L. S. Germann, P. A. Julien, I. Moudrakovski, M. Etter, T. Friščić, R. E. Dinnebier and B. V. Lotsch, *Chem.*, 2021, **7**, 1639–1652.
85 P. Kuhn, M. Antonietti and A. Thomas, *Angew. Chem., Int. Ed.*, 2008, **47**, 1639–1652.
86 J. Maschita, T. Banerjee, G. Savasci, F. Haase, C. Ochsenfeld and B. V. Lotsch, *Angew. Chem., Int. Ed.*, 2020, **59**, 15750–15758.
87 X. Guan, Y. Ma, H. Li, Y. Yusran, M. Xue, Q. Fang, Y. Yan, V. Valtchev and S. Qiu, *J. Am. Chem. Soc.*, 2018, **140**, 4494–4498.
88 M. Matsumoto, L. Valentino, G. M. Stiehl, H. B. Balch, A. R. Corcos, F. Wang, D. C. Ralph, B. J. Mariñas and W. R. Dichtel, *Chem.*, 2018, **4**, 308–317.
89 K. Dey, M. Pal, K. C. Rout, S. Kunjattu H, A. Das, R. Mukherjee, U. K. Kharul and R. Banerjee, *J. Am. Chem. Soc.*, 2017, **139**, 13083–13091.
90 R. Wang, X. Shi, A. Xiao, W. Zhou and Y. Wang, *J. Membr. Sci.*, 2018, **566**, 197–204.
91 Y. Peng, W. K. Wong, Z. Hu, Y. Cheng, D. Yuan, S. A. Khan and D. Zhao, *Chem. Mater.*, 2016, **28**, 5095–5101.
92 D. D. Medina, J. M. Rotter, Y. Hu, M. Dogru, V. Werner, F. Auras, J. T. Markiewicz, P. Knochel and T. Bein, *J. Am. Chem. Soc.*, 2015, **137**, 1016–1019.
93 A. M. Elewa, I. M. A. Mekhemer, A. F. M. EL-Mahdy, A. Sabbah, S.-Y. Chen, L.-Y. Ting, S. Abdelnaser and H.-H. Chou, *Small*, 2024, **20**, 2311472.
94 S. Koo and D. W. Kang, *CrystEngComm*, 2023, **25**, 5994–6005.
95 S.-T. Yang, J. Kim, H.-Y. Cho, S. Kim and W.-S. Ahn, *RSC Adv.*, 2012, **2**, 10179–10181.
96 W. Zhao, P. Yan, B. Li, M. Bahri, L. Liu, X. Zhou, R. Clowes, N. D. Browning, Y. Wu, J. W. Ward and A. I. Cooper, *J. Am. Chem. Soc.*, 2022, **144**, 9902–9909.

97 T. Ma, E. A. Kapustin, S. X. Yin, L. Liang, Z. Zhou, J. Niu, L.-H. Li, Y. Wang, J. Su, J. Li, X. Wang, W. D. Wang, W. Wang, J. Sun and O. M. Yaghi, *Science*, 2018, **361**, 48–52.
98 J. Han, J. Feng, J. Kang, J.-M. Chen, X.-Y. Du, S.-Y. Ding, L. Liang and W. Wang, *Science*, 2024, **383**, 1014–1019.
99 H.-S. Xu, Y. Luo, X. Li, P. Z. See, Z. Chen, T. Ma, L. Liang, K. Leng, I. Abdelwahab, L. Wang, R. Li, X. Shi, Y. Zhou, X. Fang Lu, X. Zhao, C. Liu, J. Sun and K. P. Loh, *Nat. Commun.*, 2020, **11**, 1434.
100 A. M. Evans, L. R. Parent, N. C. Flanders, R. P. Bisbey, E. Vitaku, M. S. Kirschner, R. D. Schaller, L. X. Chen, N. C. Gianneschi and W. R. Dichtel, *Science*, 2018, **361**, 52–57.
101 B. Yu, R.-B. Lin, G. Xu, Z.-H. Fu, H. Wu, W. Zhou, S. Lu, Q.-W. Li, Y. Jin, J.-H. Li, Z. Zhang, H. Wang, Z. Yan, X. Liu, K. Wang, B. Chen and J. Jiang, *Nat. Chem.*, 2024, **16**, 114–121.
102 L. Deng, W. Chen, G. Zhou, Y. Liu, L. Liu, Y. Han, Z. Huang and D. Jiang, *J. Am. Chem. Soc.*, 2024, **146**, 35427–35437.
103 C. Kang, K. Yang, Z. Zhang, A. K. Usadi, D. C. Calabro, L. S. Baugh, Y. Wang, J. Jiang, X. Zou, Z. Huang and D. Zhao, *Nat. Commun.*, 2022, **13**, 1370.
104 W. Zhang, Y. Zhang, W. Ma, X. Han, W. Gong, Y. Liu and Y. Cui, *Chem.*, 2025, **11**, 102398.
105 J. Maschita, T. Banerjee and B. V. Lotsch, *Chem. Mater.*, 2022, **34**, 2249–2258.
106 X. Kong, Z. Wu, M. Strømme and C. Xu, *J. Am. Chem. Soc.*, 2024, **146**, 742–751.
107 W.-Y. Li, J.-J. Wan, J.-L. Kan, B. Wang, T. Song, Q. Guan, L.-L. Zhou, Y.-A. Li and Y.-B. Dong, *Chem. Sci.*, 2023, **14**, 1453–1460.
108 Q. Fang, J. Wang, S. Gu, R. B. Kaspar, Z. Zhuang, J. Zheng, H. Guo, S. Qiu and Y. Yan, *J. Am. Chem. Soc.*, 2015, **137**, 8352–8355.
109 L. Bai, S. Z. F. Phua, W. Q. Lim, A. Jana, Z. Luo, H. P. Tham, L. Zhao, Q. Gao and Y. Zhao, *Chem. Commun.*, 2016, **52**, 4128–4131.
110 V. S. Vyas, M. Vishwakarma, I. Moudrakovski, F. Haase, G. Savasci, C. Ochsenfeld, J. P. Spatz and B. V. Lotsch, *Adv. Mater.*, 2016, **28**, 8749–8754.
111 G. Zhang, X. Li, Q. Liao, Y. Liu, K. Xi, W. Huang and X. Jia, *Nat. Commun.*, 2018, **9**, 2785.
112 W. Zhang, S. Xiang, Y. Han, H. Wang, Y. Deng, P. Bian, Y. Bando, D. Golberg and Q. Weng, *Biomaterials*, 2024, **306**, 122503.
113 S. Liu, C. Hu, Y. Liu, X. Zhao, M. Pang and J. Lin, *Chem. – Eur. J.*, 2019, **25**, 4315–4319.
114 S. Liu, J. Yang, R. Guo, L. Deng, A. Dong and J. Zhang, *Macromol. Rapid Commun.*, 2020, **41**, 1900570.
115 Y. Jia, L. Zhang, B. He, Y. Lin, J. Wang and M. Li, *Mater. Sci. Eng., C*, 2020, **117**, 111243.
116 R. Anbazhagan, R. Krishnamoorthi, S. Kumaresan and H.-C. Tsai, *Mater. Sci. Eng., C*, 2021, **120**, 111704.
117 F. Benyettou, N. Kaddour, T. Prakasam, G. Das, S. K. Sharma, S. A. Thomas, F. Bekhti-Sari, J. Whelan, M. A. Alkhalifah, M. Khair, H. Traboulsi, R. Pasricha, R. Jagannathan, N. Mokhtari-Soulimane, F. Gándara and A. Trabolsi, *Chem. Sci.*, 2021, **12**, 111243.
118 M. Li, Y. Peng, F. Yan, C. Li, Y. He, Y. Lou, D. Ma, Y. Li, Z. Shi and S. Feng, *New J. Chem.*, 2021, **45**, 3343–3348.
119 L. Ge, C. Qiao, Y. Tang, X. Zhang and X. Jiang, *Nano Lett.*, 2021, **21**, 3218–3224.
120 P. Gao, X. Shen, X. Liu, Y. Chen, W. Pan, N. Li and B. Tang, *Anal. Chem.*, 2021, **93**, 11751–11757.
121 Z. Zhao, J. Zhao, S. Zhang, G. Zhang, W. Chen, Z. Yang, T. Zhang and L. Chen, *Nanoscale*, 2021, **13**, 19385–19390.
122 S. Bhunia, P. Saha, P. Moitra, M. A. Addicoat and S. Bhattacharya, *Chem. Sci.*, 2022, **13**, 7920–7932.
123 B. Ma, Y. Xu, F. Hu, L. Zhai, Y. Huang, H. Qiao, J. Xiong, D. Yang, Z. Ni, X. Zheng and L. Mi, *RSC Adv.*, 2022, **12**, 31276–31281.
124 S. Das, T. Sekine, H. Mabuchi, T. Irie, J. Sakai, Y. Zhao, Q. Fang and Y. Negishi, *ACS Appl. Mater. Interfaces*, 2022, **14**, 48045–48051.
125 C. Du, W. Na, M. Shao, S. Shang, Y. Liu and J. Chen, *Chem. Mater.*, 2023, **35**, 1395–1403.
126 W.-Y. Li, J.-J. Wan, J.-L. Kan, B. Wang, T. Song, Q. Guan, L.-L. Zhou, Y.-A. Li and Y.-B. Dong, *Chem. Sci.*, 2023, **14**, 1453–1460.
127 V. Sridhar, E. Yildiz, A. Rodríguez-Camargo, X. Lyu, L. Yao, P. Wrede, A. Aghakhani, B. M. Akolpoglu, F. Podjaski, B. V. Lotsch and M. Sitti, *Adv. Mater.*, 2023, **35**, 2301126.
128 Y. Zhao, S. Das, T. Sekine, H. Mabuchi, T. Irie, J. Sakai, D. Wen, W. Zhu, T. Ben and Y. Negishi, *Angew. Chem., Int. Ed.*, 2023, **62**, e202300172.
129 Y. Zhao, T. Irie, J. Sakai, H. Mabuchi, S. Biswas, T. Sekine, S. Das, T. Ben and Y. Negishi, *ACS Appl. Nano Mater.*, 2023, **6**, 19210–19217.
130 R. Anbazhagan, T. T. V. Dinh, R. krishnamoorthi, D. Thankachan, H.-C. Tsai, Y.-H. Chang and J.-M. Yang, *Mater. Chem. Phys.*, 2024, **312**, 128612.
131 W. Zhang, S. Xiang, Y. Long, Y. Han, K. Jiang, P. Bian and Q. Weng, *ACS Appl. Mater. Interfaces*, 2024, **16**, 342–352.
132 G. Kaur and P. Kumar, *Chem. Pap.*, 2024, **78**, 3023–3032.
133 D. Fu, L. Zhong, J. Xu, A. Mo and M. Yang, *RSC Adv.*, 2024, **14**, 20799–20808.
134 F. Benyettou, N. Kaddour, T. Prakasam, G. Das, S. K. Sharma, S. A. Thomas, F. Bekhti-Sari, J. Whelan, M. A. Alkhalifah, M. Khair, H. Traboulsi, R. Pasricha, R. Jagannathan, N. Mokhtari-Soulimane, F. Gándara and A. Trabolsi, *Chem. Sci.*, 2021, **12**, 6037–6047.
135 L. Dai, F. Wu, Y. Xiao, Q. Liu, M. Meng, R. Xi and Y. Yin, *ACS Appl. Mater. Interfaces*, 2024, **16**, 17891–17903.
136 S. M. M. Moghadam, M. Ramezani, M. Alibolandi, K. Abnous and S. Mohammad Taghdisi, *J. Drug Targeting*, 2025, **33**, 1892–1901.
137 S. Yao, M. Zheng, S. Wang, T. Huang, Z. Wang, Y. Zhao, W. Yuan, Z. Li, Z. L. Wang and L. Li, *Adv. Funct. Mater.*, 2022, **32**, 2209142.
138 S. Yao, X. Zhao, X. Wang, T. Huang, Y. Ding, J. Zhang, Z. Zhang, Z. L. Wang and L. Li, *Adv. Mater.*, 2022, **34**, 2109568.

139 H. Zhu, L. Zhang, S. Tong, C. M. Lee, H. Deshmukh and G. Bao, *Nat. Biomed. Eng.*, 2019, **3**, 126–136.
140 Y. Rui, M. Varanasi, S. Mendes, H. M. Yamagata, D. R. Wilson and J. J. Green, *Mol. Ther. Nucleic Acids*, 2020, **20**, 661–672.
141 Y. He, Q. Hu, L. Wang and C. Chen, *Mater. Des.*, 2024, **237**, 112562.
142 Q. Deng, L. Zhang, X. Liu, L. Kang, J. Yi, J. Ren and X. Qu, *Chem. Sci.*, 2023, **14**, 1598–1605.
143 M. Soroushmanesh, M. Dinari and H. Farrokhpour, *Langmuir*, 2024, **40**, 19073–19085.
144 K. Yadava and A. Yadav, *RSC Pharm.*, 2025, **2**, 703–717.
145 Y. Gao, Y. Shi, M. Fu, Y. Feng, G. Lin, D. Kong and B. Jiang, *Comput. Methods Programs Biomed.*, 2020, **193**, 105493.
146 OECD (2025), Test No. 407: Repeated Dose 28-day Oral Toxicity Study in Rodents, OECD Guidelines for the Testing of Chemicals, Section 4, OECD Publishing, Paris, DOI: 10.1787/9789264070684-en.
147 Drug Products, Including Biological Products, that Contain Nanomaterials, Guidance for Industry, U.S. Department of Health and Human Services Food and Drug Administration, April 2022. https://www.fda.gov/regulatory-information/search-fda-guidance-documents/drug-products-including-biological-products-contain-nanomaterials-guidance-industry.